Dear Prof. Willy Maenhaut,

We thank you for handling our paper with your valuable time and expertise. After careful consideration of your comments, a major revision has been made to thoroughly address all your concerns.

In the revised MS (after the response letter), words marked in red indicate the contents in the original MS that have been deleted, and words marked in green (mainly including the results of PMF analysis and precipitation scavenging effect) indicate the new contents that we've added.

Below please see our point-by-point reply to your comments. We have tried to answer as detailed as possible.

Comment 1: The authors should have addressed the comments of the referees in a better way. Their reply to the second specific comment of Anonymous Referee #1 (with regard to the precipitation) makes in my opinion no sense. The approach that was used to handle this comment is much too simplistic. It is impossible that the atmospheric concentrations of elements such as V, Ni and Si are not influenced by wet scavenging.

Reply: We've made a great effort to examine the potential scavenging effect induced by precipitation on the mass concentration of ambient trace elements from the perspective of their species and sources. In brief, we found that (1) although precipitation is effective in term of reducing the overall levels of ambient trace elements, there is no uniform pattern for each elemental species; (2) there is a threshold of precipitation amount to lower ambient $PM_{2.5}$ trace elements mass; (3) trace elements contributed by sources of traffic-related (exhaust and non-exhaust) and coal combustion can be significantly removed from the atmosphere during precipitation, while this is not the case for the sources of ferrous (iron and steel) and nonferrous (Cu, Pb, Zn) metal smelting; (4) interestingly, the variations of elements concentrations contributed by shipping (mainly V and Ni) before, during, and after precipitation events were mainly governed by wind speed and direction instead of precipitation. For more details, please refer to section 3.3 in our revised MS:

3.3 Precipitation effect

Theoretically, precipitation could enhance the wet scavenging of airborne pollutants and reduce their ability to suspend because the increased moisture might capture the particles on the road surface (Kuhns et al., 2003; Karanasiou et al., 2011). Water spray (from sprinkler on road or atop tall building) to simulate natural types of precipitation has been proposed as an important abatement strategy to facilitate the reduction of ambient PM concentrations (including trace elements) in urban China (Liu et al., ,2014; Yu, 2014). However, several field measurements revealed that water spray activities did not influence PM mass levels (e.g., Karanasiou et al., 2012, 2014). Taking advantage of our simultaneous and hourly record of precipitation amount (up to 36.8 mm) and elements concentration, here we evaluate the effects of precipitation on the mitigation of $PM_{2.5}$ trace elements. The precipitation (all were in the form of rainfall) distributed during the full year of measurements is shown in Figure S13. The mass concentrations of trace elements six hours before and after precipitation events were compared from the perspective of individual species and sources. The precipitation event in this study is defined as (1) there are at least six consecutive hours with hourly rainfall amount higher than 1 mm; (2) the consecutive no-rainy time in a precipitation event should less than six hours; (3) the total no-rainy time should less than 1/3 of the entire time of a precipitation event; (4) if the rainfall amount of a specific hour is less than 0.1 mm, and there are at least three no-rainy hours before and after the rainy hour, then this hour should be treated as no-rainy hour. Consequently, 12 precipitation events during our study period were identified with the duration time and accumulated rainfall ranging from 7 to 55 hours, and 26.4 to 217.5 mm, respectively (Table S2).

3.3.1 Change of mass concentration by species

The average mass concentration of each elemental species before, during, and after every precipitation event is presented in Fig. S13. If precipitation effectively scavenge and remove aerosol, then the mass concentrations of trace elements during a precipitation event should lower than that before and after this precipitation event. However, there is no uniform variation pattern in Fig. S14, indicating that precipitation may not be the predominant factor to influence ambient elements mass in some cases. For example, most elemental species had a relatively higher mass concentration during the 12th precipitation event (lasted from 09:00 25 December to 22:00 26 December; Fig. S14). This can be explained by the much less anthropogenic activities during the periods prior to (3:00 to 8:00) and after (23:00 to 3:00 the next day) the 12th precipitation event.

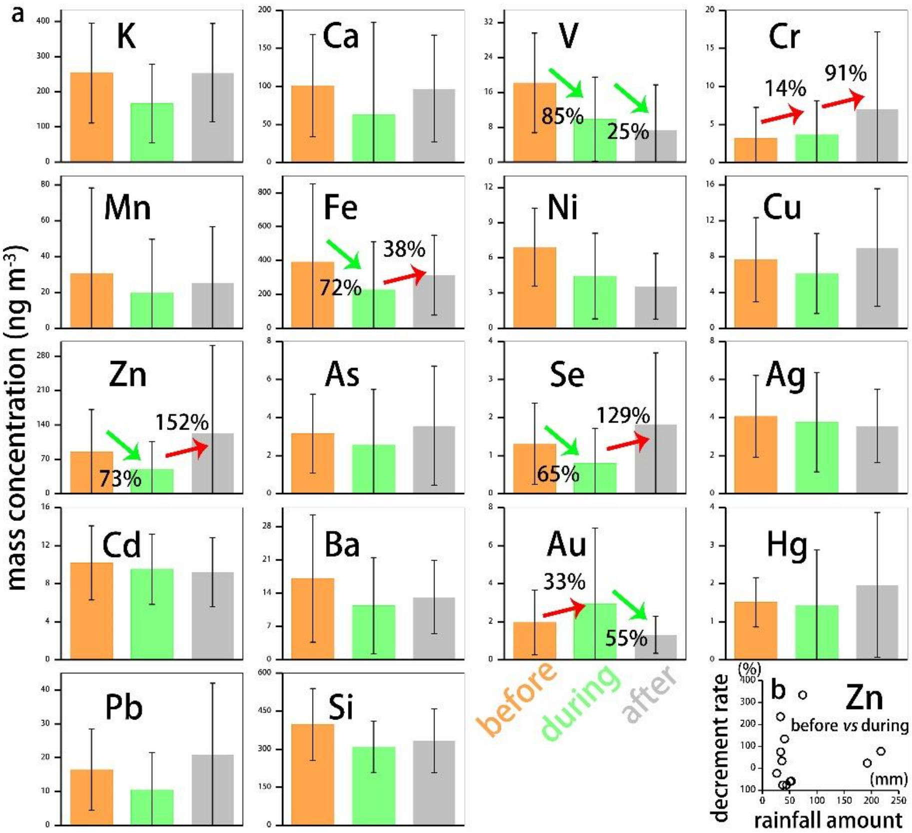

Figure 9. (**a**) The variation of the overall mass concentration of each elemental species before, during, and after the total 12 precipitation events; (**b**) scatter plot of the relationship between the rainfall amount of each precipitation event and the decrement rate of Zn concentration from the period before precipitation to the period after precipitation.

For each elemental species, the variation of mass concentration before, during, and after every precipitation event were aggregated and reported in Fig. 9a. Before precipitation events, the mass concentrations of all species except Cr and Au were higher than that during precipitation events (notably V, Zn, Fe), suggesting that water spray could generally help to reduce $PM_{2.5}$ trace elements load in the atmosphere. After precipitation events, there were six species (notably V and Au) with their mass concentrations lower than that during precipitation events, indicating potential long-lasting aftereffect of precipitation scavenging. Among all elemental species, the mass concentrations of Zn and Se fluctuate as the most ideal V-shape, which properly reflect the cycle of precipitation. However, as shown in Fig. 9b, a linear relationship cannot be observed between the decrement rate of Zn concentration and rainfall amount of each precipitation event. Although we failed to pinpoint the exact value in this study, our results imply that there is a threshold of precipitation amount to lower ambient $PM_{2.5}$ trace elements mass.

3.3.1 Change of mass concentration by sources

The variation of the overall mass concentration of trace elements contributed by each source and their relative contributions before, during, and after the total 12 precipitation events is shown in Fig. 10a to 10e, and Fig. 10f, respectively. The mass concentration of traffic-related trace elements experienced the sharpest decrease during the transition of no-rainy hours to rainy hours (159%), and a moderate rebound after precipitation (35%). Fang et al. (2015) found that mobile source emissions generated through mechanical processes (re-entrained road dust, tire and break wear) and processing by secondary sulfate were major contributors to water-soluble metals. In our study, traffic-related source mainly includes road dust and brake wear, which can not only be easily removed through precipitation but also can hardly be blown up from wet road surface after raining. In comparison, the mass contribution of coal combustion source was also wet removed rapidly first (139%) due to its tracer elements like As, Se, Pb, and Hg have larger water-soluble fraction. However, after precipitation, the contribution of coal combustion source dramatically increased over two times (Fig. 10d and 10f). This can be explained that different from traffic-related source, coal combustion-related trace elements are generally emitted through elevated chimneys in the sectors of industrial broilers and power plants. The mass concentrations of trace elements contributed by nonferrous and ferrous metal smelting during the three periods kept quite flat (Fig. 10c and 10d), suggesting that precipitation has little effect on ambient trace elements emitted from metal smelting activities. Nevertheless, given that traffic-related and coal combustion are the dominant contributors to ambient $PM_{2.5}$ trace elements, our results validate that water spray could be an effective approach to help curb the severe atmospheric metal pollution in many Chinese cities.

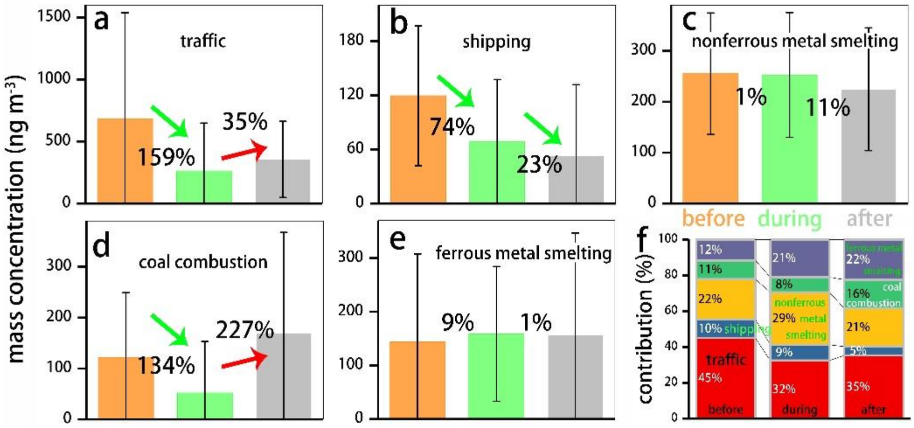

Figure 10. The variation of the overall mass concentration of trace elements contributed by traffic-related (**a**), shipping (**b**), nonferrous metal smelting (**c**), coal combustion (**d**), and ferrous metal smelting (**e**), and their relative contributions (**f**) before, during, and after the total 12 precipitation events.

In Fig. 10b and 10f, the contribution of shipping emissions to ambient trace elements (mainly V and Ni) during the three periods reduced continuously. Mostly transported from Eastern China sea, V and Ni almost exclusively originated from the east of the sampling site. In other words, the contribution of shipping emissions to urban atmosphere is supposed to be very sensitive to wind speed and wind direction in Shanghai. The wind roses for the three periods are illustrated in Fig. 11. It shows that before precipitation events, the average wind speed ($\pm 1\sigma$) was the lowest (2.3 ± 1.3 m s^{-1}), and easterly winds prevail in most times. These factors are favorable to the transportation of shipping emissions from Eastern China sea and then accumulated in Shanghai urban atmosphere. In contrast to the period before precipitation events, the average wind speed after precipitation events was the highest (3.1 ± 2.1 m s^{-1}) with northwesterly and northerly winds from mainland China can dilute shipping-related trace elements to the lowest levels (Fig. 10b). In brief, the mass concentration of shipping-related trace elements in Shanghai urban atmosphere is more likely to be influenced by winds instead of precipitation.

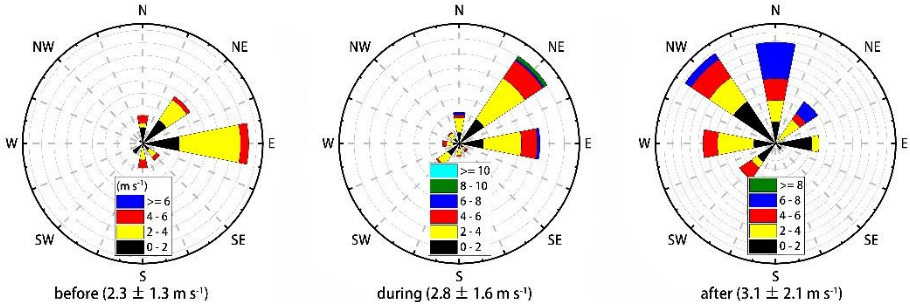

Figure 11. Wind roses plots for the periods before, during, and after the twelve precipitation events. The average wind speed (± 1σ) for each period is shown in bracket.

Comment 2: Overall, the current version of this manuscript still has serious shortcomings. 1. Although the language and grammar of the manuscript are reasonable, there is still a lot of room for improvement. Several alterations are suggested under "Further comments" below.

Reply: Thank you for your careful revision. All mistakes you mentioned regarding language and grammar in the original MS have been revised accordingly.

Comment 3: 2. The authors followed up on the suggestion of Anonymous Referee #2 to replace the word "elements" in the title by "metals". I disapprove of this change. Three of the 18 elements measured (i.e., Si, As and Se) are not metals. Si and As are metalloids and the nonmetal Se is also sometimes considered a metalloid. Also throughout the text "metal(s)" is often used where it should be "element(s)".

Reply: Agree. The full text of the MS has been thoroughly checked.

Comment 4: 3. I agree with Anonymous Referee #5 where he states that the results of the principal component analysis and also the hierarchical clustering do not bring many new insights. Still there are many sentences in the revised manuscript devoted to the results of those two approaches. It is unclear to me why did the authors did not make use of Positive Matrix Factorization (PMF) for source identification and apportionment.

thoroughly

Reply: Agree. The results of the principal component analysis and the hierarchical clustering have been deleted in the revised MS. Alternatively, positive matrix factorization (PMF) was applied to identify and apportion the sources of trace elements in $PM_{2.5}$ fraction. Five different factors were resolved (notable elements and relative contribution in brackets): traffic-related (Ca, Fe, Ba, Si; 46%), shipping (V, Ni; 6%), nonferrous metal melting (Ag, Cd, Au; 15%), coal combustion (As, Se, Hg, Pb; 18%), and ferrous metal smelting (Cr, Mn, Zn; 15%). Each factor has been vigorously validated by various evidences. Please see below for more information:

3.2 Source analysis

In the PMF analysis, three to ten factor solutions were initially examined, from which possible solutions (i.e., four to six factor solutions) were chosen based on the change of Q/Q_{exp}, the achievement of the constant and global minimum of Q, the displacement of factor elements, and the interpretation of physically meaningful factors (Text S1; see discussion later). The most reliable solution was explained by five factors. The chemical profiles and average contributions of the five factors are illustrated in Fig. 4 with the time-series evolution of these factors included in the Supplement (Fig. S9). On the one hand, we will use various mathematical and physical criteria to constrain different solutions of source apportionment. On the other hand, we will take CPF and BPP as diagnostic tools for quickly gaining the idea of potential source regions, which in turn will contribute to further analysis of source apportionment. Ultimately, the five factors were assigned to different sources, i.e., traffic-related, shipping, nonferrous metal smelting, coal combustion, and ferrous metal smelting.

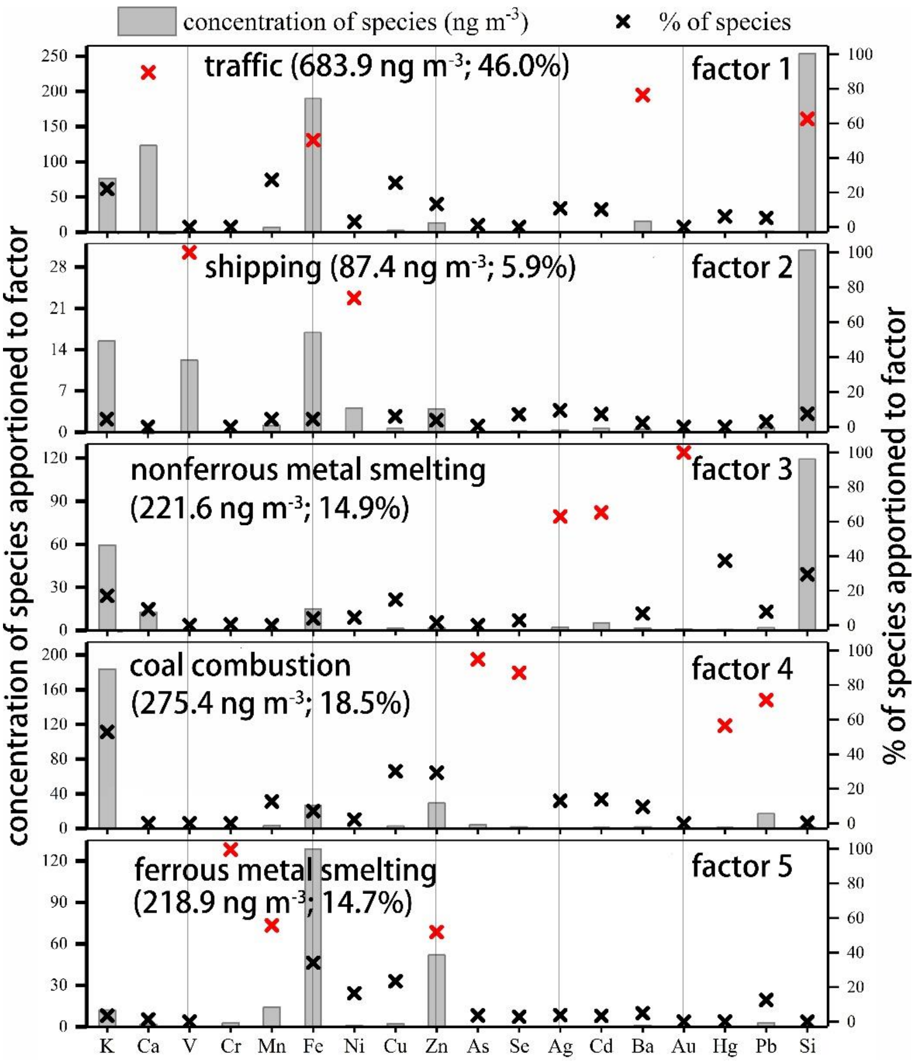

Figure 4. PMF-resolved source profiles (concentration and % of species apportioned to factor) and average contributions (in the parentheses) of individual sources to measured total $PM_{2.5}$ elements in Shanghai. The notable species for each factor/source are marked in red.

3.2.1 Traffic-related

Factor 1 was characterized by a large mass fraction of Ca, Fe, Ba, and Si, which explained 89.5%, 50.3%, 76.5%, and 62.6% of the variation, respectively. This mixed factor is similar to that reported by Amato et al. (2009, 2013), Bukowiecki et al. (2010), Harrison et al. (2012), and Visser et al. (2015b). In urban atmosphere, Fe can be released from engine oil or catalyst equipped gasoline vehicles (Chen et al., 2007). Besides, Fe is linked to non-exhaust emissions such as brake wear because it is the support material for brake pads, and the agents present in brake linings typically consist of Ba, Mn and Cu (Lough et al., 2005; Hjortenkrans et al., 2007; Dall'Osto et al., 2016). Therefore, Fe and Ba can be regarded as chemical tracers for traffic-related source (exhaust and non-exhaust) (Thorpe et al., 2008; Lin et al., 2015). Ca and Si are known as two of the most abundant elements in the upper continental crust, and their atmospheric origins typically attributed to wind-blown dust. Located on the eastern coast of China, Shanghai rarely receives long-range transport of crustal matters from aeolian dust and the Gobi Desert in northwestern China (Huang et al., 2013). Sampling in the urban area of Shanghai, airborne Ca and Si should be dominated by anthropogenic activities like road fugitive dust or urban construction works. In Fig. S10, significant correlations are observed for Ca, Si, Fe, and Ba, suggesting that the measured Ca and Si during our study period were more likely derived from road fugitive dust. Therefore, factor 1 can be assigned to traffic-related source and it was the largest source in Shanghai, accounting for 46.0% (683.9 ng m^{-3}) of the total measured elemental mass in $PM_{2.5}$.

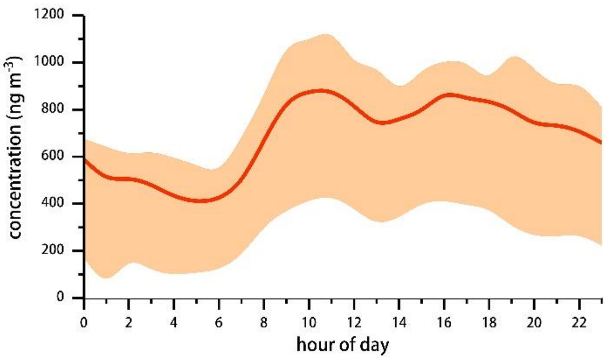

Figure 5. Diurnal variation of PMF-derived elemental concentration for factor 1. The red line, bottom boundary, and upper boundary represent the mean, 1st quartile, and 3rd quartile of the concentration value, respectively.

Hourly measurements over one-year periods provide a unique opportunity to examine the diurnal profile of factor 1. As reported in Fig. 5, the concentration of trace elements contributed by factor 1 shows a marked bimodal diurnal cycle, with average values at rush hours are over two times higher than at nighttime. Such variation pattern agrees well with the diurnal variation of traffic flow in Shanghai (Chang et al., 2016a), further confirming that factor 1 can be interpreted as traffic-related emissions.

3.2.2 Shipping

In Fig. 4, V (100%) and Ni (74%) comes almost exclusively from factor 2, while factor 2 contributes to less than 10% of any other elemental species. V is typically emitted from oil and petrochemical refining and combustion, and natural gas extraction and processing (Duce and Hoffman, 1976; Hope, 1994; Shafer et al., 2012). From CPF and BPP analysis (Fig. S11), higher concentrations of both V and Ni were observed when winds originated from east, northeast, and southeast directions. The most dominant directions were east and southeast, suggesting the influence from costal port cluster or petroleum refinery industry located east/southeast of Shanghai (Fig. 1). Gathering evidence revealed that the ratio of V/Ni can be served as a robust indicator of shipping emissions (Tao et al., 2013; Celo et al., 2015; Liu et al., 2017; Viana et al., 2009). Recent study in Shanghai port suggested that the ratio of V/Ni in aerosols emitted from heavy oil combustion of ocean-going ship engines was 3.4 on average (Zhao et al., 2013). Here measured in urban area, the average ratio of V/Ni in our study was 3.1 with slightly seasonal changes (Fig. 6), indicating V- and Ni-containing aerosols from shipping emissions subject to minor atmospheric transformation. In short, factor 2 likely corresponds to shipping emissions (instead of petrochemical refining), which is consistent with the results of many previous source apportionment works (e.g., Liu et al., 2017; Zhao et al., 2013; Cesari et al., 20014; Healy et al., 2010).

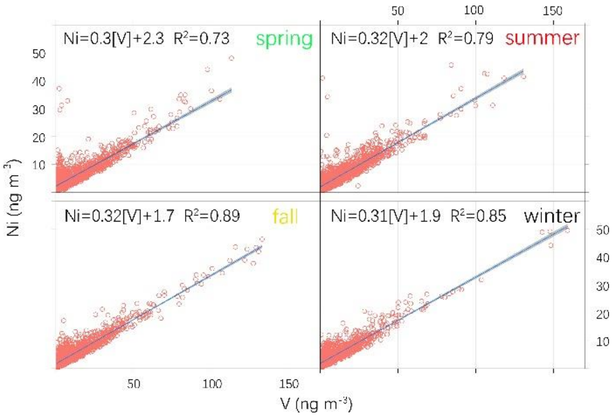

Figure 6. Linear correlation analysis between V (x axis) and Ni (y axis) in Shanghai during four seasons.

Although shipping emissions only contribute to 5.9% of trace elements in Shanghai urban center, its share can be expected to greatly increase in harbor district (Zhao et al., 2013). The good news is that since 1 January 2016, the sea areas of Shanghai and its neighboring ports were designed as shipping emission control area, requiring use of lower sulfur fuels in place of heavy fuel oil in main engines of ships (Zhen et al., 2018). Therefore, it is critically important to assess the impacts of fuel changes on air quality in Shanghai in the future through continuous measurements of trace elements.

3.2.3 Nonferrous metal smelting

The predominant elements found in factor 3 were Au (100%), Cd (65%), and Ag (63%) with 37% of Hg. These four heavy metals are important associated elements in Cu, Pb, and Zn ores. In fact, Cu, Pb, and Zn smelting represent the three most common form of nonferrous metal smelting in China (Tian et al., 2015). Because of high temperatures during roasting, sintering and smelting process for the extraction of Cu, Pb, and Zn from ores, metals like Au, Cd, Ag, and Hg in nonferrous metal ores will inevitably be vaporized and released into the flue gas (Pacyna and Pacyna, 2001; Wu et al., 2012). Therefore, factor 3 was interpreted as nonferrous metal smelting emissions and the contribution of this factor was 14.9% (221.6 ng m^{-3}) to total measured elemental mass in $PM_{2.5}$.

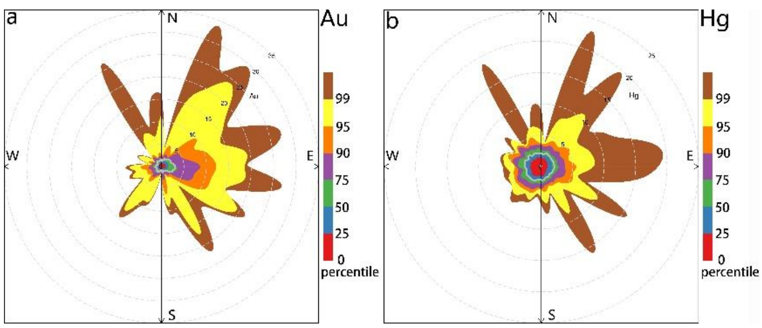

Figure 7. Percentile rose plot of Au (**a**) and Hg (**b**) concentrations in Shanghai between March 2016 and February 2017. The percentile intervals are shaded and shown by wind direction.

To further pinpoint the specific subsector of nonferrous metal smelting, here we calculate percentile concentration levels of Au and Hg, and plot them by wind direction in Fig. 7 (and Ag, Cd in Fig. S12). It clearly shows Au and Hg largely share the same source region that different from Ag and Cd, indicating that Au and Hg were emitted from a similar subsector of nonferrous metal smelting.

In Shanghai, Zn smelting is the most important contributor of Hg emissions from the nonferrous metal smelting sector. Therefore, element Au resolved in factor 3 during our study period can be expected to be originated from Zn smelting.

3.2.4 Coal combustion

The most abundant elements found in factor 4 were As, Se, Pb, Hg (explaining 56% to 95% of the variation) with some contributions of Cu (30%), Zn (29%) and unexpected large amount of K (53%). As, Se, Pb, Hg, and Cu are typical marker elements for coal combustion. In China, 73% of As, 62% of Se, 56% of Pb, and 47% of Hg were found to be emitted from coal combustion. Coal consumption in southern China (including Shanghai) is mainly driven by industrial boilers and power plant, while in norther China, coal-based heating is also a major sector of coal consumption (Tian et al., 2015). Seasonally, the average mass concentration of coal combustion-related $PM_{2.5}$ trace elements during winter (407 ng m^{-3}) was much higher than that during spring (296 ng m^{-3}), summer (148 ng m^{-3}), and fall (210 ng m^{-3}) (Fig. 8). This seasonal pattern was not observed for other sources (not shown). Shanghai has a humid subtropical climate and experiences four distinct seasons. Winters are chilly and damp, with northwesterly winds from norther China can transport air pollutants (including trace elements) caused by coal-based heating to Shanghai atmosphere (Huang et al., 2013; Chang et al., 2017). As the largest city-scale coal consumer in China, coal combustion contributed to 275.4 ng m^{-3} or 18.5% of $PM_{2.5}$ trace elements during our study period.

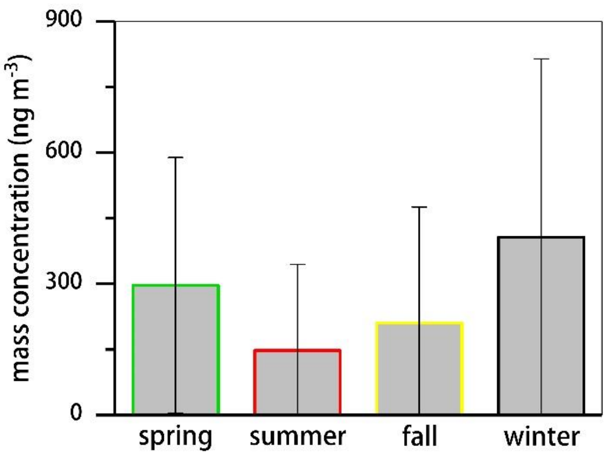

4

Figure 8. Seasonal variation of elements concentrations contributed by coal combustion in Shanghai. The error bar indicates one standard derivation.

Traditionally, K in particles was considered to be originated from biomass burning along with some contribution of fugitive dust (Zhang et al., 2010; Hueglin et al., 2005; Fang et al., 2015). Here we show that over half of element K in urban Shanghai were derived from coal combustion. The reason for this discrepancy maybe that in most previous studies, K in particles was pretreated using deionized water to extract (Wang et al., 2013b). In fact, K has high mineral affinity (elements associated with aluminosilicates, carbonates and other minerals in coal ash), and in some extreme cases, only about 1% of K in fly ash from coal combustion can be extracted by water (Querol et al., 1996). For example, particles collected from coal combustion by Wang et al. (2013b) were extracted with deionized water, then atomized and measured by an ATOFMS. The ATOFMS mass spectrum contained relatively low K peak. The observation by Wang et al. (2013) was not consistent with that of Suess et al. (2002), in which they detected larger K peaks in ATOFMS spectra for coal combustion particles in an in situ measurement (i.e. freshly emitted particles were directly introduced into ATOFMS and measured).

3.2.5 Ferrous metal smelting

Factor 5 was distinguished by high levels of Cr, Mn, and Zn representing 100%, 56%, and 52% of the explained variation, respectively. These elements are typically emitted from ferrous metal smelting. For example, the steel production industry represents the dominant contributor to Zn emissions, accounting for about 60% in China (Tian et al., 2015). Driven by rapid modernization of its infrastructure and manufacturing industries, China produced more than 49% of world steel production in 2017 (around 830 million tons), and 6 of 10 of the largest steel producers are in China (data retrieved from https://www.worldsteel.org). Headquartered in Shanghai (20 km northwest of the sampling site), the Baosteel is the fifth-largest steel producer in the world measured by crude steel output, with an annual output of around 35 million tons. Meanwhile, there are several factories of ferrous metal processing located in western Shanghai (Fig. 1). Since element Cr is reported to be transported over distances by air flow (Perry et al., 1999), the presence of ferrous metal smelting activities in the west/northwest of the sampling site is inferred to be associated with this factor based on the results of CPF and BBP in Fig. 9. Overall, ferrous metal smelting contributed 218.9 ng m^{-3} or 14.7% of $PM_{2.5}$ trace elements in Shanghai.

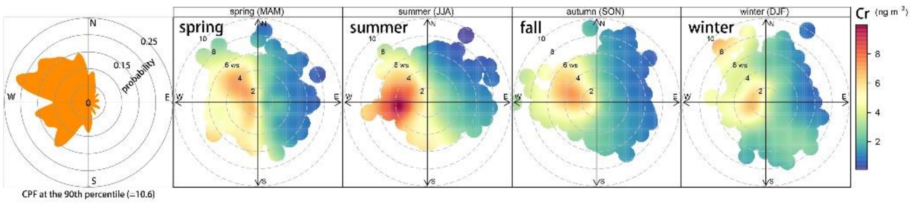

Figure 9. Conditional probability function analysis (left) and bivariate polar plots (right) of seasonal concentrations (in ng m^{-3}) of Cr in Shanghai between March 2016 and February 2017. The center of each plot (centered at the sampling site) represents a wind speed of zero, which increases radially outward. The concentration is shown by the color scale.

5.3 Precipitation effect

Theoretically, precipitation could enhance the wet scavenging of airborne pollutants and reduce their ability to suspend because the increased moisture might capture the particles on the road surface (Kuhns et al., 2003; Karanasiou et al., 2011). Water spray (from sprinkler on road or atop tall building) to simulate natural types of precipitation has been proposed as an important abatement strategy to facilitate the reduction of ambient PM concentrations (including trace elements) in urban China (Liu et al., ,2014; Yu, 2014). However, several field measurements revealed that water spray activities did not influence PM mass levels (e.g., Karanasiou et al., 2012, 2014). Taking advantage of our simultaneous and hourly record of precipitation amount (up to 36.8 mm) and elements concentration, here we evaluate the effects of precipitation on the mitigation of $PM_{2.5}$ trace elements. The precipitation (all were in the form of rainfall) distributed during the full year of measurements is shown in Figure S13. The mass concentrations of trace elements six hours before and after precipitation events were compared from the perspective of individual species and sources. The precipitation event in this study is defined as (1) there are at least six consecutive hours with hourly rainfall amount higher than 1 mm; (2) the consecutive no-rainy time in a precipitation event should less than six hours; (3) the total no-rainy time should less than 1/3 of the entire time of a precipitation event; (4) if the rainfall amount of a specific hour is less than 0.1 mm, and there are at least three no-rainy hours before and after the rainy hour, then this hour should be treated as no-rainy hour. Consequently, 12 precipitation events during our study period were identified with the duration time and accumulated rainfall ranging from 7 to 55 hours, and 26.4 to 217.5 mm, respectively (Table S2).

Comment 5: 4. The concentration data in lines 28-31 and in lines 316-319 (and on some other occasions in the manuscript) contain too many significant figures. Two significant figures suffice in case the first significant figure is larger or equal than 2, and when the first significant figure equals 1, three significant figures can be used.

Reply: Revised accordingly.

Comment 6: 5. Section 2.2.1: I presume that hourly concentration data were used in the statistical analyses. If so, this should clearly be indicated.

Reply: Indicated as your suggestion in the revised MS.

Comment 7: 6. Lines 479-480: Considering that up to nearly 9000 data points were available for each element (if hourly concentration data were used in the statistical analyses), how can the authors make the statement that "much larger datasets are required for definitive source apportionment with PCA"? Even in case daily averages were used in the PCA, then there would still be sufficient data for an appropriate PCA.

Reply: Agree. PCA analysis has been deleted in the revised MS.

Comment 8: Further comments for the Main text:

Lines 26 and 126: What is meant by "reactive filter"? In line 193 it is mentioned that a Teflon filter tape was used in the Xact instrument. Teflon filters are typically not reactive at all.

Reply: Sorry for the confusion. There "reactive filter" essentially means "moving filter" because filter can be automatically advanced into the analysis area. To avoid misunderstanding, "reactive filter" has been replaced as "Teflon filter".

Comment 9: Line 34: Replace "with other" by "with that in other".

Line 35: Replace "in sites" by "at sites".

Line 44: Replace "sourced from" by "derived from".

Line 213: Replace "at PMC" by "at the PMC".

Line 226: Replace "for species of" by "for".

Line 228: Replace "than other" by "than those of other".

Line 248: Replace "principle component" by "principal component".

Line 257: The acronym "PCA" was already defined in line 248. Its should not be defined again.

Line 303: Replace "has described" by "has been described".

Line 305: Replace "3 Results" by "3. Results".

Line 310: Replace "illustrated in" by "presented in".

Line 334: Replace "accounting for" by "accounts for".

Line 356: Replace "willalso" by "will also".

Line 363: Replace "were also illustrated in" by "are shown in".

Line 378: Replace "winter were" by "winter is".

Line 383: Replace "later)" by "below)".

Line 387: Why is reference made here to the wind speed? There is no information about the wind speed in Fig. 6c.

Line 394: Replace "can be served" by "can serve".

Line 400: Replace "well as" by "well as for".

Line 402: Replace "evening" by "in the evening".

Line 414: Replace "from other" by "from that of other".

Line 415: Replace "and 16:00" by "and at 16:00".

Line 416: Replace "were primarily" by "are primarily".

Line 417: Replace "were more" by "are more".

Line 421: Replace "matters" by "matter".

Line 439: Replace "be primarily sourced" by "primarily originate".

Line 441: Replace "of Cu origins" by "of the Cu origin".

Line 454: Replace "and presented" by "and they are presented".

Lines 456-457: Replace "trace crustal matters" by "crustal matter".

Line 458: Replace "trace crustal matters" by "the crustal matter trace elements".

Line 461: Replace "trace crustal matters" by "crustal matter elements".

Lines 471-473: There is something wrong with the wind directions given here. It seems to me that "west" in line 471 should be replaced by "east" and "southwest" in line 473 by "southeast".

Line 473: Replace "are sourced from " by "originated from".

Line 478: Replace "Explore and constrain more" by "Exploration and constraining of more".

Line 489: Replace "later)" by "below)".

Line 490: Replace "Matrix reorder" by "Matrix reordering".

Line 505: Replace "illustrated in" by "presented in".

Line 511: Replace "Even though" by "Nevertheless".

Line 517: Replace "illustrated in" by "shown in".

Line 529: It is unclear to me what is meant by "reaming".

Line 552: Replace "matters from" by "matter from".

Line 554: Replace "be sourced from" by "originate from".

Line 560: Replace "principle source" by "principal source".

Lines 573-574: Replace "approximately 20 km apart" by "at approximately 20 km".

Line 575: Replace "also evidently reflects" by "also indicates".

Line 597: Replace "e.g." by "i.e.".

Line 624: Insert ", Edinburgh, United Kingdom," after "Hydrology".

Lines 648-658: "Carslaw and Ropkins, 2012" should come before "Carslaw et al., 2006".

Line 844: Replace "Inventory" by "inventory".

Line 1001: Replace "A collection of" by "Overview of".

Line 1008: Replace "although a huge" by "a huge" and replace "had been" by "has been".

Line 1009: Replace "in which no" by "but that no".

Line 1017: Replace "A land use" by "Land use".

Page 34, Figure 2: The unit for the abscissa data ("value") in the right part of the figure should be specified.

Line 1034: Replace "A quick glance of the mass" by "Average mass".

Page 37, Figure 5d: Replace "weakday" by "weekday" in the abscissa.

Page 38, caption of Figure 6, line 2: There is no information about the wind direction in the Figure.

Page 44, Figure 12: The unit for the data in the abscissas and ordinates should be specified. The data in several cells for V, Ni, Ag and Cd are not readable, although for some of them a significance level of "***" is specified. Then, in the last line of the figure caption, 6 p-values are given and only 5 symbols; besides, it is unclear what the last of these 5 symbols really is.

Page 46, Figure 14: It should be indicated that this figure shows component loadings. Furthermore, in the caption of the figure "Principle component" should be replaced by "Principal component".

Page 48, Figure 16: The unit for the concentration data in this figure should be specified.

Comment for the Supplement:

Caption of Table S1: Replace "Inter-comparison of trace metals" by "Inter-comparison between ICP-MS and Xact for trace elements".

Reply: We were deeply touched by your careful revision, thanks!

All the comments above have been revised accordingly in the revised MS.

First long-term and near real-time measurement of trace elements in China's urban atmosphere: temporal variability, source apportionment, and precipitation effect

Yunhua Chang[1, 2], Kan Huang[3], Mingjie Xie[4], Congrui Deng[3], Zhong Zou[5], Shoudong Liu[1, 2], and Yanlin Zhang[1, 2 *]

[1]Yale-NUIST Center on Atmospheric Environment, International Joint Laboratory on Climate and Environment Change (ILCEC), Nanjing University of Information Science & Technology, Nanjing 210044, China

[2]Key Laboratory of Meteorological Disaster, Ministry of Education (KLME)/ Collaborative Innovation Center on Forecast and Evaluation of Meteorological Disasters (CIC-FEMD), Nanjing University of Information Science & Technology, Nanjing 210044, China

[3]Center for Atmospheric Chemistry Study, Shanghai Key Laboratory of Atmospheric Particle Pollution and Prevention (LAP[3]), Department of Environmental Science and Engineering, Fudan University, Shanghai 200433, China

[4]School of Environmental Science and Engineering, Nanjing University of Information Science & Technology, Nanjing 210044, China

[5]Pudong New Area Environmental Monitoring Station, Shanghai 200135, China

Correspondence to: Yanlin Zhang (dryanlinzhang@outlook.com or zhangyanlin@nuist.edu.cn)

Abstract: Atmospheric trace elements, especially metal species, are an emerging environmental and health concern with insufficient understanding of their levels and sources in Shanghai, the most important industrial megacity in China. Here we continuously performed a one-year (from March 2016 to February 2017) and hourly-resolved measurement of eighteen elements in fine particles ($PM_{2.5}$) at Shanghai urban center with a Xact multi-metals monitor and several collocated instruments.

~~Independent ICP-MS offline analysis of filter samples was used to validate the performance of Xact that was based on energy-dispersive X-ray fluorescence analysis of aerosol deposits on Teflon filter tapes.~~ Mass concentrations (mean±1σ; ng m^{-3}) determined by Xact ranged from detection limits (nominally 0.1 to 20 ng m^{-3}) to 15 μg m^{-3}. ~~with Si as the most abundant element (639±1005), followed by Fe (406±385), K (388±326), Ca (192±383), Zn (120±131), Mn (32±39), Pb (27±26), Ba (24±25), V (13±14), Cu (12±11), Cd (10±4), As (7±7), Ni (6±5), Cr (4.5±6), Ag (4±2.6), Se (2.6±2.9), Hg (2.2±1.7), and Au (2.2±3.4).~~ Elements related oxidized species comprised an appreciable fraction of $PM_{2.5}$ during all seasons, accounting for 8.3% on average. As a comparison, atmospheric elements concentration level in Shanghai was comparable with that in other industrialized cities in East Asia but one or two orders of magnitude higher than at sites in North America and Europe. ~~Various mathematical methods and high resolution measurement data provided the criteria to constrain various solutions of source identification. The results showed that atmospheric trace element pollution in Shanghai was due to the interplay of local emissions and regional transport. Different sources of metal species generally have different temporally-evolving patterns associated with different source regions. Specifically, V and Ni were confirmed as the prominent and exclusive tracers of heavy oil combustion from shipping traffic. Fe and Ba were strongly related to brake wear, and exhibited a significant correlation with Si and Ca, suggesting that Si and Ca in Shanghai were primarily sourced from road fugitive dust rather than long-distance dust transport and local building construction sites. Stationary combustion of coal was found to be the major source of As, Se, Pb, Cu and K, and the ratio of As/Se was used to infer that coal consumed in Shanghai likely originated from Henan coal fields in Northern China. Cr, Mn and Zn were the mixed result of emissions from stationary combustion of coal, ferrous metals production, and nonferrous metals processing. Ag and Cd in Shanghai urban atmosphere were also the mixture of miscellaneous sources.~~ Positive matrix factorization (PMF) was applied to identify and apportion the sources of elements in $PM_{2.5}$ mass. Five different factors were resolved (notable elements and relative contribution in brackets): traffic-related (Ca, Fe, Ba, Si; 46%), shipping (V, Ni; 6%), nonferrous metal melting (Ag, Cd, Au;

15%), coal combustion (As, Se, Hg, Pb; 18%), and ferrous metal smelting (Cr, Mn, Zn; 15%). Contributed by exhaust and non-exhaust vehicle emissions, traffic-related factor shows strong bimodal diurnal profile with average concentration over two times higher during rush hour than during nighttime. Shipping factor was firmly identified because V and Ni, two recognized tracers of shipping emissions, almost exclusively transported from East China Sea and their ratio (around 0.31) fallen within the variation range of V/Ni in particles emitted from heavy oil combustion. Interestingly, nearly half of K were derived from coal combustion with high mineral affinity (elements associated with aluminosilicates, carbonates and other minerals in coal ash). The contributions of (non)ferrous metal smelting to trace elements are consistent with a newly-developed emission inventory. Although the precipitation scavenging effect on the mass concentration of trace elements varied among different species and sources, precipitation could effectively lower traffic- and coal combustion-related trace elements. Therefore, water spray to simulate natural types of precipitation could be one of the abatement strategies to facilitate the reduction of ambient $PM_{2.5}$ trace elements in urban atmosphere. Collectively, our findings in this study provide baseline levels and sources of trace elements with high detail, which are needed for developing effective control strategies to reduce the high risk of acute exposure to atmospheric trace elements in China's megacities.

1 Introduction

It is well known that personal exposure to atmospheric aerosols have detrimental consequences and aggravating effects on human health such as respiratory, cardiovascular, and allergic disorders (Pope III et al., 2002; Pope III et al., 2009; Shah et al., 2013; West et al., 2016; Burnett et al., 2014). Among the chemical components relevant for aerosol health effects, airborne heavy metals (a very imprecise term without authoritative definition (John, 2002), loosely refers to elements with atomic density greater than 4.5 g cm^{-3} (Streit, 1991)) are of particular concern as they typically feature with unique properties of bioavailability and bioaccumulation (Morman and Plumlee, 2013; Tchounwou et al., 2012; Fergusson, 1990; Kastury et al., 2017), representing 7 of the 30 hazardous air pollutants identified by the US Environmental Protection Agency (EPA) in terms of posing the greatest potential health threat in urban areas (see www.epa.gov/urban-air-toxics/urban-air-toxic-pollutants). Depending on aerosol composition, extent and time of exposure, previous studies have confirmed that most elements components of fine particles ($PM_{2.5}$; particulate matter with aerodynamic diameter equal to or less than 2.5 μm) exerted a multitude of significant diseases from pulmonary inflammation, to increased heart rate variability, to decreased immune response (Fergusson, 1990; Morman and Plumlee, 2013; Leung et al., 2008; Hu et al., 2012; Pardo et al., 2015; Kim et al., 2016).

Guidelines for atmospheric concentration limits of many trace elements are provided by the World Health Organization (WHO) (WHO, 2005). In urban atmospheres, ambient trace elements typically represent a small fraction of $PM_{2.5}$ on a mass basis, while elements species like Cd, As, Co, Cr, Ni, Pb and Se are considered as human carcinogens even in trace amounts (Iyengar and Woittiez, 1988; Wang et al., 2006; Olujimi et al., 2015). It has been shown that Cu, Cr, Fe and V have several oxidation states that can participate in many atmospheric redox reactions (Litter, 1999; Brandt and van Eldik, 1995; Seigneur and Constantinou, 1995; Rubasinghege et al., 2010a), which can catalyze the generation of reactive oxygenated species (ROS) that have been associated with direct molecular damage and with the induction of biochemical synthesis pathways (Charrier and Anastasio, 2012; Strak et al., 2012; Rubasinghege et al., 2010b; Saffari et al., 2014; Verma et al., 2010; Jomova and Valko, 2011). Additionally, lighter elements such as Si, Al and Ca are the most abundant crustal elements next to oxygen, which can typically constitute up to 50% of elemental species in remote continental aerosols (Usher et al., 2003; Ridley et al., 2016). These species are usually associated with the impacts of aerosols on respiratory diseases and climate (Usher et al., 2003; Tang et al., 2017).

Health effects of airborne elements species are not only seen from chronic exposure, but also from short-term acute concentration spikes in ambient air (Kloog et al., 2013; Strickland et al., 2016; Huang et al., 2012). In addition, atmospheric emissions, transport, and exposure of trace elements to human receptors may depend upon rapidly evolving meteorological conditions and facility operations (Tchounwou et al., 2012; Holden et al., 2016). Typical ambient trace elements sampling devices collect 12 to 24-hr integrated average samples, which are then sent off to be lab analyzed in a time-consuming and labor-intensive way. As a consequence, daily integrated samples inevitably ignore environmental shifts with rapid temporality, and thereby hinder the efforts to obtain accurate source apportionment results such as short-term elements pollution spikes related to local emission sources. In fact, during a short-term trace elements exposure event, 12 or 24-hr averaged sample concentrations for elements species like Pb and As may be one order of magnitude lower than the 4-hr or 15-min average concentration from the same day (Cooper et al., 2010). Current source apportionment studies are mainly performed by statistical multivariate analysis such as receptor models (e.g., Positive Matrix Factorization, PMF), which could greatly benefit from high inter-sample variability in the source contributions through increasing the sampling time resolution. In this regard, continuous monitoring of ambient elements species on a real-time scale is essential for studies on trace elements sources and their health impacts.

Currently, there are only a few devices available for the field sampling of ambient aerosols with sub-hourly or hourly resolution, i.e., the Streaker sampler, the DRUM (Davis Rotating-drum Unit for Monitoring) sampler, and the SEAS (Semi-continuous Elements in Aerosol Sampler) (Visser et al., 2015b; Visser et al., 2015a; Bukowiecki et al., 2005; Chen et al., 2016). Mass loadings of trace elements collected by these samplers can be analyzed with highly sensitive accelerator-based analytical techniques, in particular particle-induced X-ray emission (PIXE) or synchrotron radiation X-ray fluorescence (SR-XRF) (Richard et al., 2010; Bukowiecki et al., 2005; Maenhaut, 2015; Traversi et al., 2014). More recently, Aerosol Time-Of-Flight Mass Spectrometry (ATOFMS) (Murphy et al., 1998; Gross et al., 2000; DeCarlo et al., 2006), National Institute for Standards and Technology (NIST)-traceable reference aerosol generating method (QAG) (Yanca et al., 2006), distance-based detection in a multi-layered device

(Cate et al., 2015), environmental magnetic properties coupled with support vector machine (Li et al., 2017), and Xact^{TM} 625 automated multi-metals analyzer (Fang et al., 2015; Jeong et al., 2016; Phillips-Smith et al., 2017; Cooper et al., 2010) have been developed for more precise, accurate, and frequent measurement of ambient elements species. The Xact method is based on nondestructive XRF analysis of aerosol deposits on reactive filter tapes, which has been validated by US Environmental Technology Verification testing and several other field campaigns (Fang et al., 2015; Phillips-Smith et al., 2017; Jeong et al., 2016; Yanca et al., 2006; Cooper et al., 2010; Park et al., 2014; Furger et al., 2017).

Located at the heart of the Yangtze River Delta (YRD), Shanghai is home to nearly 25 million people as of 2015, making it the largest megacity in China (Chang et al., 2016). Shanghai city is one of the main industrial centers of China, playing a vital role in the nation's heavy industries, including but not limited to, steel making, petrochemical engineering, thermal power generation, auto manufacture, aircraft production, and modern shipbuilding (Normile, 2008; Chang et al., 2016; Huang et al., 2011). Shanghai is China's most important gateway for foreign trade, which has the world's busiest port, handling over 37 million standard containers in 2016 (see www.simic.net.cn/news_show.php?lan=en&id=192101). As a consequence, Shanghai is potentially subject to substantial quantities of trace elements emissions (Duan and Tan, 2013; Tian et al., 2015). Ambient concentrations of trace elements, especially Pb and Hg, in the Shanghai atmosphere have been sporadically reported during the past two decades (Shu et al., 2001; Lu et al., 2008; Wang et al., 2013a; Zheng et al., 2004; Huang et al., 2013; Wang et al., 2016). Of current interest are V and Ni, which are often indicative of heavy oil combustion from ocean-going vessels (Fan et al., 2016; Liu et al., 2017). However, previous work rarely presented a full spectrum of elements species in ambient aerosols. Furthermore, recent attribution of hospital emergency-room visits in China to $PM_{2.5}$ constituents failed to take short-term variations of trace elements into account (Qiao et al., 2014), which could inevitably underestimate the toxicity of aerosols and potentially misestimate the largest influence of aerosol components on human health effects (Honda et al., 2017).

In this study, the first of its kind, we conducted a long-term and near real-time measurement of atmospheric trace elements in $PM_{2.5}$ with a Xact multi-metals analyzer in Shanghai, China, from March 2016 to February 2017. The primary target of the present study is to elucidate the atmospheric abundances, variation patterns and source contributions of trace elements in a complex urban environment, which can be used to support future health studies. The primary target of the present study is to elucidate the levels and sources of atmospheric trace elements in a complex urban environment, which can be used to support future health studies. Meanwhile, the potential effect of precipitation scavenging on the mass concentration of trace elements will be investigated to examine if water spay could be proposed as an effective approach to curb severe trace elements pollution in China's urban atmosphere.

2 Methods

2.1 Field measurements

2.1.1 Site description

Figure 1a shows the map of eastern China with provincial borders and land cover, in which Shanghai city (provincial level) sits in the middle portion of China's eastern coast and its metropolitan area (indicated as the densely-populated area in Fig. 1b) concentrated on the south edge of the mouth of the Yangtze River. The municipality borders the provinces of Jiangsu and Zhejiang to the north, south and west, and is bounded to the east by the East China Sea (Fig. 1a). Shanghai has a humid subtropical climate and experiences four distinct seasons. Winters are chilly and damp, with northwesterly winds from Siberia which can cause nighttime temperatures to drop below freezing. Air pollution in Shanghai is low compared to other cities in northern China, such as Beijing, but still substantial by world standards, especially in winter (Han et al., 2015; Chang et al., 2017).

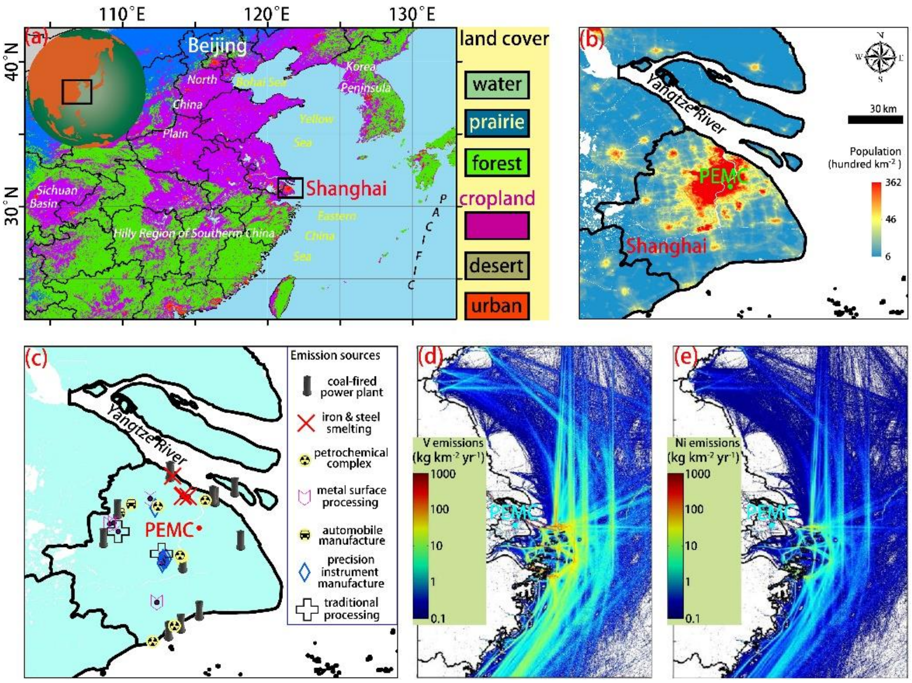

Figure 1. Land use map indicating the location of Shanghai (**a**; black box), as well as the population density (**b**) and the major point sources (**c**) around the sampling site (PEMC). The emissions of V (**d**) and Ni (**e**) from shipping in the YRD and the East China Sea within 400 km of the coastline were estimated based on an automatic identification system model (adopted from Fan et al. (2016)).

Field measurements were performed at the rooftop (~18 m above ground level) of Pudong Environmental Monitoring Center (PEMC; 121.5447°E, 31.2331°N; ~7 m above sea level) in Pudong New Area of southwestern Shanghai, a region with dense population (Fig. 1b). Pudong New Area is described as the "showpiece" of modern China due to its height-obsessed skyline and export-oriented economy. For PEMC, there were no metal-related sources (except for road traffic) or high-rise buildings nearby to obstruct observations, so the air mass could flow smoothly. More broadly, as indicted in Fig. 1c, PEMC is surrounded by a multitude of emissions sources such as coal-fired power plants (CFPP) in all directions and iron and steel smelting in the northwest. Furthermore, a high level of ship exhaust emissions in 2010 such as V (Fig. 1d) and Ni (Fig. 1e) in the YRD and the East China Sea within 400 km of China's coastline was recently quantified based on an automatic identification system model

(Fan et al., 2016). Therefore, PEMC can be regarded as an ideal urban receptor site of diverse emission sources. More information regarding the sampling site has been given elsewhere (Chang et al., 2017; Chang et al., 2016).

2.1.2 Hourly elemental species measurements

From March 1st 2016 to February 28th 2017, hourly ambient mass concentrations of eighteen elements (Si, Fe, K, Ca, Zn, Mn, Pb, Ba, V, Cu, Cd, As, Ni, Cr, Ag, Se, Hg, and Au) in $PM_{2.5}$ were determined by a Xact multi-metals monitor (Model Xact™ 625, Cooper Environmental Services LLT, OR, USA) (Phillips-Smith et al., 2017; Jeong et al., 2016; Fang et al., 2015; Yanca et al., 2006). Specifically, the Xact sampled the air on a reel-to-reel Teflon filter tape through a $PM_{2.5}$ cyclone inlet (Model VSCC-A, BGI Inc., MA, USA) at a flow rate of 16.7 L min^{-1}. The resulting $PM_{2.5}$ deposit on the tape was automatically advanced into the analysis area for nondestructive energy-dispersive X-ray fluorescence analysis to determine the mass of selected elemental species as the next sampling was being initiated on a fresh tape spot. Sampling and analysis were performed continuously and simultaneously, except during advancement of the tape (~20 sec) and during daily automated quality assurance checks. For every event of sample analysis, the Xact included a measurement of pure Pd as an internal standard to automatically adjust the detector energy gain. The XRF response was calibrated using thin film standards for each elements of interest. These standards were provided by the manufacturer of Xact, produced by depositing vapor phase elements on blank Nuclepore (Micromatter Co., Arlington, WA, USA). The Nuclepore filter of known area was weighed before and after the vapor deposition process to determine the concentration (μg cm^{-2}) of each element. In this study, excellent agreement between the measured and standard masses for each element was observed, indicating a deviation of $< 5\%$. The 1-hr time resolution minimum detection limits (in ng m^{-3}) were: Si (17.80), K (1.17), Ca (0.30), V (0.12), Cr (0.12), Mn (0.14), Fe (0.17), Ni (0.10), Cu (0.27), Zn (0.23), As (0.11), Se (0.14), Ag (1.90), Cd (2.50), Au (0.23), Ba (0.39), Hg (0.12), and Pb (0.13).

As a reference method to validate the Xact on-line measurements, daily $PM_{2.5}$ samples were also collected at the PEMC site using a four-channel aerosol sampler (Tianhong, Wuhan, China) on 47 mm cellulose acetate and glass fiber filters at a flow rate of 16.7 L min^{-1}. The sampler was operated once a week with a 24-hr sampling time (starting from 10:00 am). In total 48 filter samples (26 cellulose acetate filter samples and 22 glass fiber filter samples) were collected, in which 8 paired samples were simultaneously collected by cellulose acetate and glass fiber filters. In the laboratory, elemental analysis procedures strictly followed the latest national standard method "Ambient air and stationary source emission-Determination of metals in ambient particulate matter-Inductively coupled plasma/mass spectrometer (ICP-MS)" (HJ 657-2013) issued by the Chinese Ministry of Environmental Protection. A total of 24 elements (Al, Fe, Mn, Mg, Mo, Ti, Sc, Na, Ba, Sr, Sb, Ca, Co, Ni, Cu, Ge, Pb, P, K, Zn, Cd, V, S, and As) were measured using Inductively coupled plasma-mass spectrometer (ICP-MS; Agilent, CA, USA). The results of the 8 paired samples were first compared. Significant correlations were observed for K, Cr, Mn, Fe, Ni, Cu, As, Cd, Ba, Zn, and Pb (Table S1), and these species were used to validate the performance of Xact. In Table S1, the slope values of Cr (1.9) and Ba (2.6) were higher than those of other species, this can be explained by higher background values of Cr and Ba collected by the cellulose acetate filters.

2.1.3 Auxiliary measurements, quality assurance and quality control

~~Hourly mass concentrations of PM2.5 were measured using a Thermo Fisher Scientific TEOM 1405-D. Data on hourly concentrations of CO, NO2, and SO2 were provided by PEMC.~~ Meteorological data, including ambient temperature (*T*), relative humidity (RH), wind direction (WD) and wind speed (WS), were provided by Shanghai Meteorological Bureau at Century Park station (located approximately 2 km away from PEMC). The routine procedures, including the daily zero/standard calibration, span and range check, station environmental control, and staff certification, followed the Technical Guideline of Automatic Stations of Ambient Air Quality in Shanghai based on the national specification HJ/T193–2005. This was modified from the technical guidance established by the USEPA. QA/QC for the Xact measurements was implemented throughout the campaign. The internal Pd, Cr, Pb, and Cd upscale values were recorded after the instrument's daily programmed test, and the PM_{10} and $PM_{2.5}$ cyclones were cleaned weekly.

2.2 Data analysis

~~2.2.1 Statistical analysis~~

~~To identify possible sources of measured trace metals, three methods of statistical analysis, i.e., correlation matrix, principle component analysis (PCA), and hierarchical clustering of reordering correlation matrix, were performed. The "corrplot" package in R is a graphical display of a correlation matrix, confidence interval. It also contains specific algorithms to calculate matrices. More information regarding corrplot can be found at CRAN.R-project.org/package=corrplot (Wei and Simko, 2016).~~

~~Spearman correlations were firstly performed to establish correlations between trace metals, which can be used to investigate the dependence among multiple metal species at the same time. The result is a table containing the correlation coefficients between each variable and the distribution of each metal species on the diagonal. Secondly, principle component analysis (PCA) with a varimax rotation (SPSS Statistics® 24, IBM®, Chicago, IL, USA) was performed on the measured data set, which has been used widely in receptor modelling to identify major source categories. The technique operates on sample-to-sample fluctuations of the normalized concentrations. It does not directly yield concentrations of species from different sources but identifies a minimum number of common factors for which the variance often accounts for most of the variance of species (e.g., Venter et al. (2017) and references therein). The trace metal concentrations determined for the 18 species were subjected to multivariate analysis of Box-Cox transformation and varimax rotation, followed by subsequent PCA. Lastly, we applied an agglomeration strategy for hierarchical clustering, a method of cluster analysis which seeks to build a hierarchy of clusters, to mine the hidden structure and pattern in the correlation matrix (Murdoch and Chow, 1996; Friendly, 2002). In order~~

to decide which clusters should be combined as a source, or where a cluster should be split, a measure of dissimilarity between sets of observations is required. Ward's method is served as a criterion applied in hierarchical cluster analysis. The "corrplot" package can draw rectangles around the chart of the correlation matrix (indicated as a potential source) based on the results of hierarchical clustering. Readers can refer to https://cran.r-project.org/web/packages/corrplot/corrplot.pdf and https://cran.r-project.org/web/packages/corrplot/vignettes/corrplot-intro.html for details regarding the manual and demonstration of hierarchical clustering, respectively.

2.2.1 Positive Matrix Factorization (PMF) analysis for source apportionment

The Positive Matrix Factorization or PMF is an effective source apportionment method to identify and quantify possible emission sources of measurements using the bilinear factor model (Paatero and Tapper, 1994)

$$x_{ij} = \sum_{k=1}^{p} g_{ik} f_{kj} + e_{ij}, \qquad (1)$$

where x_{ij} is the j^{th} species concentration measured in the i^{th} sample, g_{ik} is the contribution of the k^{th} source to the i^{th} sample (factor time series) and f_{kj} is the concentration of the j^{th} species in the kth source (factor profiles). The part of the data remaining unexplained by the model is represented by the residual matrix e_{ij}. The entries of g_{ik} and f_{kj} (required to be non-negative) are fit using a least-squares algorithm that iteratively minimizes the objective function Q:

$$Q = \sum_{i=1}^{n} \sum_{j=1}^{m} \left(\frac{e_{ij}}{\sigma_{ij}} \right)^2 . \qquad (2)$$

where σ_{ij} are the measurement uncertainties.

In this work, the US Environmental Protection Agency (EPA) PMF version 5.0 was applied to attribute $PM_{2.5}$ trace elements to specific factors/sources. One-year hourly-resolved measurements (n = 8784) of eighteen elements in $PM_{2.5}$ fraction were obtained and included for PMF analysis. The measurements (n = 1265) with all elements missed were excluded. An estimated fractional uncertainty of 10% was used to derive the uncertainty data set (Kim et al., 2005; Kim and Hopke, 2007), which did not impact the interpretability of the PMF results. The missing values of individual elements were replaced by their geometric mean of the remaining observations, and their accompanying uncertainties were set to four times the geometric mean. The measurements below detection limit (BDL) were set to half the detection limit, with uncertainties set at five-sixths the detection limit (Polissar et al. 1998). The EPA PMF 5.0 has three uncertainty estimation methods, including bootstrapping (BS), displacement (DISP), and bootstrapping enhanced with DISP (BS-DISP) (Norris et al., 2014; Brown et al., 2015; Paatero et al., 2014; Wang et al., 2017). BS-DISP analysis is time consuming due to the huge data set (7519 × 18), and only BS and DISP analysis were conducted individually. Details of the uncertainty analysis are described in the supporting information (Text S1). In this study, PMF solutions using 3-10 factors were considered, and the final factor number is determined based on the interpretability as well the uncertainty analysis with BS and DISP methods.

2.2.2 Conditional probability function and bivariate polar plot for tracing source regions

The determination of the geographical origins of trace elements in Shanghai requires the use of diagnostic tools such as the conditional probability function (CPF) and bivariate polar plot (BPP), which are very useful in terms of quickly gaining an idea of source impacts from various wind directions and have already been successfully applied to various atmospheric pollutants and pollution sources (Chang et al., 2017; Carslaw and Ropkins, 2012). In this study, the CPF and BPP were performed on the one-year data set for the major trace elements with similar source. The two methods have been implemented in the R "openair" package and are freely available at www.openair-project.org (Carslaw and Ropkins, 2012).

The CPF is defined as CPF = m_θ/n_θ, where m_θ is the number of samples in the wind sector θ with mass concentrations greater than a predetermined threshold criterion, and n_θ is the total number of samples in the same wind sector. CPF analysis is capable of showing which wind directions are dominated by high concentrations and with which probability. In this study, the 90th percentile of a given element species was set as threshold, and 24 wind sectors were used ($\Delta\theta = 15^0$). Calm wind (< 1 m s^{-1}) periods were excluded from this analysis due to the isotropic behavior of the wind vane under calm winds.

The BPP demonstrates how the concentration of a targeted species varies synergistically with wind direction and wind speed in polar coordinates, which thus is essentially a non-parametric wind regression model to alternatively display pollution roses but include some additional enhancements. These enhancements include: plots are shown as a continuous surface and surfaces are calculated through modelling using smoothing techniques. These plots are not entirely new as others have considered the joint wind speed-direction dependence of concentrations (see for example Liu et al. (2015)). However, plotting the data in polar coordinates and for the purposes of source identification is new. The BPP has described in more detail in Carslaw et al. (2006) and the construction of BPP has been presented in our previous work (Chang et al., 2017).

3 Results and discussion

3.1 Mass concentrations

The temporal patterns and summary statistics of hourly elemental species concentrations determined by the Xact at PEMC during March 2016-Feburary 2017 are presented in Fig. 2. The mass concentrations of the 18 elements measured in Shanghai were sorted from high to low in Fig. 3. The one-year data set presented in the current study, to the best of our knowledge, represents the longest on-line continuous measurement series of atmospheric trace elements.

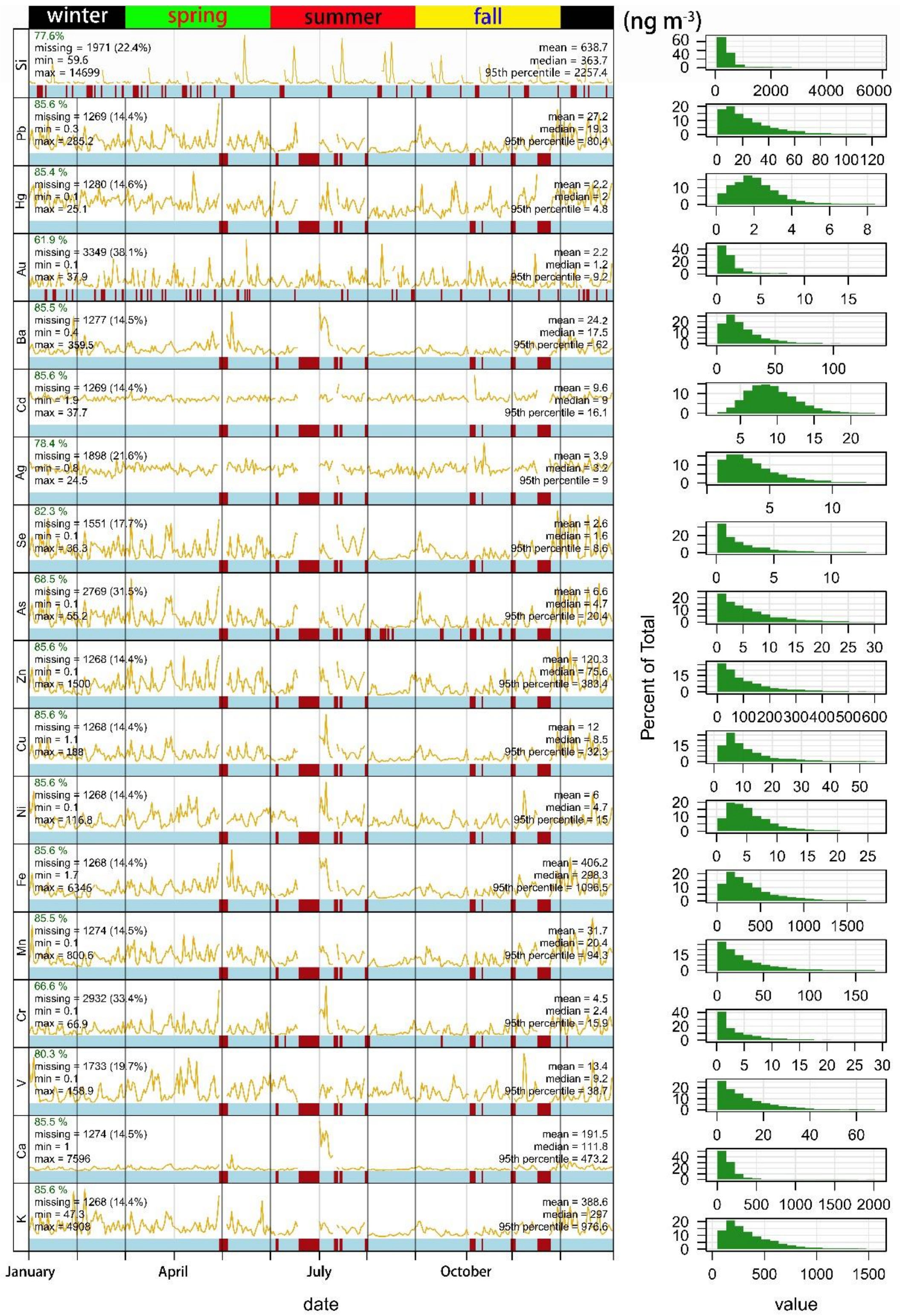

Figure 2. General statistical summaries of 18 trace elements measured in Shanghai. The plots in the left panel show the time series data, where blue shows the presence of data and red shows missing data. The mean daily values are also shown in pale yellow scaled to cover the range in the data from zero to the maximum daily value. As such,

the daily values are indicative of an overall trend rather than conveying quantitative information. For each elemental species (at hourly resolution), the overall summary statistics are given. The panels on the right show the distribution of each elemental species using a histogram plot.

Taking the study period as a whole, ambient average mass concentrations of elemental species varied between detection limit (ranging from 0.05 to 20 ng m^{-3}) and nearly 15 μg m^{-3}, with Si as the most abundant element (mean ± 1σ; 638.7 ± 1004.5 ng m^{-3}), followed by Fe (406 ± 385 ng m^{-3}), K (389 ± 326 ng m^{-3}), Ca (192 ± 383) ng m^{-3}, Zn (120 ± 131 ng m^{-3}), Mn (32 ± 39 ng m^{-3}), Pb (27 ± 26 ng m^{-3}), Ba (24 ± 25 ng m^{-3}), V (13 ± 15 ng m^{-3}), Cu (12 ± 11 ng m^{-3}), Cd (10 ± 4 ng m^{-3}), As (7 ± 7 ng m^{-3}), Ni (6 ± 5 ng m^{-3}), Cr (5 ± 6 ng m^{-3}), Ag (4 ± 2.6 ng m^{-3}), Se (2.6 ± 2.9 ng m^{-3}), Hg (2.2 ± 1.7 ng m^{-3}), and Au (2.2 ± 3.4 ng m^{-3}). According to the ambient air quality standards of China (GB 3095-2012), EU (DIRECTIVE 2004/107/EC) and WHO, the atmospheric concentration limits for Cd, Hg, As, Cr (VI), Mn, V, and Ni are 5, 50 (1000 for WHO), 6 (6.6 for WHO), 0.025, 150 (WHO), 1000 (WHO), and 20 (25 for WHO) ng m^{-3}, respectively. Therefore, airborne metal pollution in Shanghai is generally low by the current limit ceilings. Nevertheless, information regarding the specific metal compounds or chemical forms is rarely available given that most analytical techniques only record data on total metal content. In the absence of this type of information, it is generally assumed that many of the elements of anthropogenic origin (especially from combustion sources) are present in the atmosphere as oxides. Here we reconstructed the average mass concentrations of metal and crustal oxides as 5.2, 5.0, 2.8, and 3.1 μg m^{-3} in spring, summer, fall, and winter, respectively, while the annual average concentration as 3.9 μg m^{-3}, which accounting for 8.3% of total $PM_{2.5}$ mass (47 μg m^{-3}) in 2016. Detailed calculation of the reconstructed mass has been fully described elsewhere (Dabek-Zlotorzynska et al., 2011).

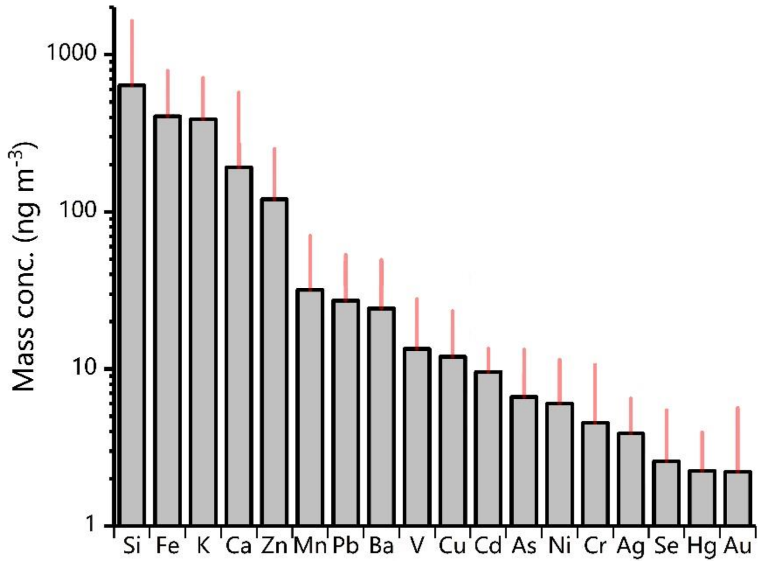

Figure 3. Average mass concentrations of 18 trace elements measured in Shanghai as sorted from high to low (log10 scaling). The dark red line indicates one standard deviation.

Table 1. Overview of long-term and high-time resolution measurements of ambient trace elements concentrations (ng m^{-3}) in fine particles.

Species	Shanghai, CN[a]	Gwangju, KP[b]	London, UK[c]	London, UK[d]	Barcelona, ES[e]	Wood Buffalo, CA[f]	Toronto, CA[g]
Ag	3.9	/	/	/	/	/	/
As	6.6	9.6	/	/	/	/	/
Au	2.2	/	/	/	/	/	/
Ba	24.2	52.0	10.3	3.7	/	/	1.9
Ca	191.5	122	78.7	50.1	130.0	54.0	54.0
Cd	9.6	/	/	/	/	/	/
Cr	4.5	/	2.3	0.8	8.0	0.04	0.24
Cu	12.0	15.5	12.8	4.9	8.0	2.04	3.1
Fe	406.2	293.0	350.3	118.9	131.0	60.0	76.8
Hg	2.2	/	/	/	/	/	/
K	388.6	732.0	27.2	23.7	82.0	31.0	27.1
Mn	31.7	24.0	4.8	2.5	6.0	1.12	1.8
Ni	6.0	3.8	0.5	0.2	3.0	0.08	0.21
Pb	27.2	49.0	2.3	1.8	12.0	/	2.4
Se	2.6	4.3	/	/	/	/	0.3
Si	638.7	/	/	/	/	143	/
V	13.4	4.6	1.3	0.6	8.0	0.21	0.11
Zn	120.3	103.0	8.9	5.3	25.0	0.88	11.3

Note: a, this study; b, Park et al., 2014; c, $PM_{0.3\text{-}2.5}$, Marylebone Road (Visser et al., 2015b); d, $PM_{0.3-2.5}$, North Kensington (Visser et al., 2015b); e, Road site (Dall'Osto et al., 2013); f, Phillips-Smith et al., 2017; g, Sofowote et al., 2015. We noticed that although a huge data set of hourly resolved trace metals had been reported in Jeong et al. (2016) and Visser et al. (2015a), but that no detailed information regarding the specific mass concentrations of trace elements were given.

The toxicological effect of hazardous elements species is more evident and well known in soils and aquatic ecosystems, while few (if any) studies on the geochemical cycle of trace metals have considered the fast dynamics of trace elements in the atmosphere. Using a diversity of chemical, physical, and optical techniques, elevated atmospheric concentrations of various element species have been observed globally; however, a tiny minority of them were performed with high time resolution. As a comparison, we compiled previous work related to the near real-time measurements of trace elements concentrations in Table 1. The concentrations of most trace elements in Shanghai were commonly an order or two orders of magnitude higher than those measured in Europe and North America, and generally ranged in the same level as industrialized city like Kwangju in South Korea. Exceptionally, the concentrations of V and Ni in Shanghai were up to three times higher than that of Kwangju City. This is expected since Shanghai has the world's busiest container port, and V and Ni were substantially and almost exclusively emitted from heavy oil combustion in ship engines of ocean-going vessels (see more discussion in Section 3.2 and 3.3).

In contrast to traditional trace elements measurements, the on-line XRF used in the current study enables measurement of elements species concentrations with 1 hr resolution, which are useful both for source discrimination and in determining the processes contributing to elevated trace elements levels through investigation of their seasonal, weekly, weekday-weekend, and diurnal cycles (Fig. S2-S8; see discussion below).

~~We willalso discuss weekly cycles because certain emission sources may make a pause or reduction during weekends. Additionally, Shanghai has a humid subtropical climate~~

and experiences four distinct seasons, which could potentially exert an influence on the mass concentrations of atmospheric metal species. Therefore, monthly and seasonal variations of ambient concentrations for each metal species were demonstrated. The variations in meteorology, including T, RH, wind speed, wind direction, and precipitation, at PEMC during our study period were also illustrated in Fig. S1.

As depicted in Fig. 4, the seasonally-averaged mass concentrations of Ag and Cd stayed exceptionally constant regardless of the season. Moreover, variations of Ag and Cd in Fig. 5 are highly consistent on a weekly and diurnal basis, both exhibiting a sharp increase of (normalized) mass concentrations after midnight and then an outright decline after 1:00 (local time), and keeping quite steady during the rest of the day. Globally, anthropogenic emissions of Ag and Cd exceed the natural rates by well over an order of magnitude (Nriagu, 1996; Nriagu, 1979). Thus, our results strongly signaled that Ag and Cd pollution in highly populous Shanghai had very stable and climate-independent anthropogenic emission sources.

Except for Ag and Cd, other metal species were seasonally variable without a uniform variation pattern (Fig. 4). Specifically, the concentrations of five metal species, i.e., As, Cu, Hg, K, and Pb, were higher in winter and lower in summer, which were consistent with the seasonal variation pattern of aerosol organics, sulphate, nitrate, and ammonium that were fully explored in China. Generally, severer air pollution in Eastern China during winter were mainly attributed to the accumulation of pollutants emitted from coal-based heating in conjunction with stagnant meteorological conditions (Huang et al., 2013). However, other trace metals like Ba, Cr, Fe, Mn, Ni, V, and Zn showed the highest concentrations in spring, suggesting more complex sources and different physical/chemical formations of atmospheric metal species in Shanghai (see discussion later). A better example is Ca and Si, which exhibited the highest degree of seasonal variations with higher concentration levels in summer.

As with Ag and Cd, another example of covariation is V and Ni (Fig. 6). Diurnally, both V and Ni peaked at around 6:00 and then gradually decreased to the bottom at 14:00, which were generally in agreement with wind speed (Fig. 6c), suggesting that V- and Ni-containing aerosols in Shanghai undergo mid- to long-range atmospheric transport. Co-emitted from heavy oil combustion, previous studies in Shanghai port have concluded that a ratio of 3.4 for V/Ni in ambient aerosols could be a reliable indicator of a ship traffic source. Here performed in urban area, the average ratio of V/Ni in our study was 3.1 with slightly seasonal changes (Fig. 7), which was very close to the ratio of averaged V and Ni content in ship heavy fuel oils, indicating V- and Ni-containing aerosols subject to minor atmospheric transformation and thus can be served as a robust tracer of shipping emissions even in costal urban areas. The office hours for Shanghai customs is Monday through Saturday, and the most important holiday in the Chinese Calendar-Lunar New Year is usually celebrated during February. This can be used to explain why the weekly (monthly) lowest impact of shipping emissions in Shanghai occurred during Sunday (Fig. 6d) (February (Fig. 6c)).

Distinctive diurnal variation patterns are observed for Si, Ca, Fe, Ba (Fig. 8) as well as Mn and Zn (Fig. 9), characterized by two marked peaks at noon (10:00-11:00) and evening (17:00-18:00), and agreeing well with the diurnal variation of Shanghai traffic flow. Indeed, as the largest megacity in terms of economy and population in China, the contribution of vehicles, both exhaust and non-exhaust emissions (Thorpe and Harrison, 2008), to ambient trace metals cannot be understated in Shanghai. As demonstrated in Fig. 8d and Fig. 9d, there is an evident drop in the concentrations of Si, Ca, Fe, Ba, Mn and Zn after the start of the weekends. Data collected from Shanghai Traffic Administration Bureau, Fig. S2 shows seasonally average weekly cycles of on-road traffic flow in Shanghai, in which the average traffic flows in weekends were lower than during weekdays. Given that Fe is the support material for brake pads, and the agents present in brake linings typically consist of Zn, Mn and Ba, less traffic flow in weekends not only lowers re-suspended road dust but also reduces metal species emissions (Zhao et al., 2015; Xie et al., 2008). Nevertheless, the monthly variation pattern of Si was different from other metals during April through June (Fig. 8c), and Ca exhibited unusually high levels in July (Fig. 8c) and 16:00 (Fig. 8b). PMF analysis of elemental species has suggested that Fe and Ba in urban atmospheres were primarily caused by vehicular brake wear while high levels of Si and Ca were more likely driven by road resuspended dust (Heo et al., 2009; Harrison et al., 2012; Jeong et al., 2016; Amato et al., 2011; Xie et al., 2008). Besides, construction activities are always thriving in China, which have been confirmed as an important source of Si- and Ca-rich crustal matters (Tian et al., 2015). Building construction activities in Shanghai are concentrated between the end of the spring festival (normally the end of February) and the approach of midsummer heat (August) (Tian et al., 2015). For an annual mean of 16.1 °C, Shanghai averages 28.3 °C in August, and the municipal authority will impose a mandatory moratorium toward outdoor construction once temperature rises to 37 °C (Chang et al., 2016). Besides, heavy-duty diesel vehicles (mostly for transporting and dumping construction waste) in Shanghai can only be allowed to operate after midnight (Chang et al., 2016), leading to higher emissions from diesel engines and unpaved roads.

In Fig. 10 and Fig. 11, diurnal variations of trace metals like Cu, K, Se, As, Pb, Au, and Hg are seemingly full of clutter. Interestingly however, the monthly and weekly cycles of the above-mentioned metal species are remarkably consistent, suggesting the possibility of sharing similar sources. Apart from anthropogenic activity, the planetary boundary layer height in Shanghai normally reaches its annual maximum during August and September (Chang et al., 2016), which are favorable to the vertical dispersion of air pollutants, leading to the lowest concentration levels in Fig. 10. From a perspective of man-made emissions, coal combustion of industrial boilers and nonferrous metal smelting represent the dominant sources for Se/As/Pb/Cr, and Au/Hg, respectively. China annually emits around 10000 metric tons Cu, which have long been thought to be primarily sourced from automotive braking because copper or brass is a major ingredient in friction material (Tian et al., 2015). However, our results based on field measurements in Shanghai go against the inherent notion of Cu origins. Gathering evidence has shown that topsoil and coal ash are also enriched in K (Schlosser, et al., 2002; Thompson and Argent, 1999; Westberg et al., 2003; Reff et al., 2009). These findings suggest more diverse sources of trace metals in a highly industrialized megacity like Shanghai.

3.2 Source analysis

The goal of source analysis in the current study is twofold. On the one hand, we will use various mathematical and physical criteria to constrain different solutions of source apportionment. On the other hand, we will take CPF and BPP as diagnostic tools for quickly gaining the idea of potential source regions, which in turn will contribute to further analysis of source apportionment.

3.2.1 Pinpoint the best possible source

As the first approach in the source analysis, Spearman correlation matrixes were prepared for all measured elemental species and presented in Fig. 12. From Fig. 12, relatively good correlations are observed between trace metals associated with heavy oil combustion (i.e., V and Ni), brake and tire wear (e.g., Fe, Mn, Ba and Zn), trace crustal matters (i.e., Si and Ca), and coal combustion (e.g., Se, As and Pb), indicating the complex influence of multiple sources in Shanghai. Still, trace crustal matters are also well correlated with metal species related to brake and tire wear. As discussed in Section 3.1, the bimodal variations of Si and Ca are also evident, which jointly suggest that the trace crustal matters we observed in Shanghai urban atmosphere were primarily derived from road fugitive dust. Nevertheless, with approximately 70% of most of the airborne crustal species being present in the coarse size fraction (Huang et al., 2013), here we call for more size-resolved sampling and analysis of PM to provide a more detailed understanding of atmospheric trace metals in the future.

Using multiple lines of evidence above, we have inferred heavy oil combustion from ship engines as the possible source of V and Ni. As shown in Fig. 12, in contrast to all other inter-correlated trace metals, V and Ni are not only highly correlated but also exclusively correlated to each other. For metal species data greater than their 90th percentile, CPF analysis in Fig. 13 shows that over 90% Ni and almost all V observed in our receptor site come from the west (East China Sea). From a perspective of geographical origin, Fig. 13 also clearly shows major air masses containing both V and Ni are sourced from the southwest. Overall, it can be safely concluded that shipping emissions are the most likely source of V and Ni in Shanghai. The successful identification of the most likely source, i.e., shipping emissions, is helpful in terms of examining the feasibility of various source apportionment solutions. In other words, V and Ni should be clustered as a single factor/source in any solution.

3.2.2 Explore and constrain more sources

To determine sources of more trace metals, PCA was applied as an exploratory tool, since much larger datasets are required for definitive source apportionment with PCA. Therefore, only the most apparent groupings of metal species relating to expected sources in the region were identified. The factor loadings are presented in Fig. 14, indicating six statistically significant factors with eigenvalues equal to or greater than 1. These six factors obtained explained nearly 80% of the variance. Unexpectedly, PCA of the 18 elemental species did not reveal any meaningful factors. This can be preliminarily tested by the large contribution of V and Ni in two different factors, but more importantly, was attributed to the large influence of nonferrous smelting, coal combustion, and traffic-related emissions on ambient trace metals measured at PEMC (see discussion later).

Matrix reorder in conjunction with clustering analysis can be a powerful tool for mining the hidden structure and pattern in the correlation matrix of Fig. 12. Here six solutions of source apportionment, from 3 sources/factors to 8 sources/sources, determined by clustering analysis are presented in Fig. 15. As mentioned above, we can rule out the solution of 3 and 4 sources/factors in Fig. 15a and 15b at first since V and Ni are combined with Au and Hg as a single source.

In Fig. 15c through 15f, Au and Hg are always clustered together as an individual factor, suggesting certain similar source(s) they may share. Globally, anthropogenic sources, including a large number of industrial point sources, annually account for 2320 Mg of

Hg released to the atmosphere (Nriagu, 1996). Despite various estimates of emission levels among different studies, Hg emissions from nonferrous metal production, coal consumption by industrial boilers and coal combustion by power plants incontrovertibly represent the top three anthropogenic sources in China, with a share of 33.1, 25.4 and 20.7% for each sector according to Tian et al. (2015). In other words, stationary combustion of coal contributes roughly half of Hg emissions of anthropogenic origins. The distribution of metal-related factories is illustrated in Fig. 1, in which coal fired power plants encompass our site from all directions while nonferrous metal-related works are concentrated in the west (especially in the northwest) but absent in the east of PEMC. Here we calculate percentile concentration levels of Au and Hg, and plot them by wind direction in Fig. 16a and 16b, respectively. It clearly shows Au and Hg are primarily derived from stationary combustion of coal because the overwhelmingly prevailing air masses are from the west of PEMC. Even though, there are few 99-99.9th percentile data that are originated from the northwest of PEMC (Fig. 16a and 16b), signaling that nonferrous metals production only affect high percentile concentrations of Au and Hg at PEMC.

Statistically, the relatively weak correlation between Ag and Cd (Fig. 12) excludes the possibility that they could equally share the same source. Therefore, the solution of 5 factors/sources illustrated in Fig. 15c is superficially invalid. A knowledge gap remains regarding the emissions of Ag in China, while this is not the case for Cd. In total ~456 metric tons in 2010, the major category sources for Cd emissions in China were nonferrous metals smelting (mainly primary Cu smelting industry), coal consumption by industrial boilers and other non-coal sources, which accounted for 44.0, 22.8 and 8.4% of the total emissions, respectively (Tian et al., 2015). Significantly high concentrations of Ag were also observed near the field of nonferrous metals processing works and coal-fired power plants in China, suggesting that nonferrous metal production and industrial coal consumption are also important sources of Ag. As reported in Fig. 16c and 16d, the receptor site, PEMC, evenly receives air masses containing Ag and Cd in all directions, indicating that both Ag and Cd in the Shanghai urban atmosphere are the mixture of miscellaneous sources.

Among the reaming metal species, Cu/K/Pb/As/Se, Cr/Mn/Zn, Fe/Ba, and Ca/Si are grouped together as a population from first to last in Fig. 15. In China, 73% of As, 62% Se, 56% of Pb, and 50% Cu emissions were found to be coal combustion (Tian et al., 2015). Therefore, As and Se are typically treated as the specific tracers of coal-related emissions in China (Tian et al., 2015; Zhang, 2010; Ren, 2006). Different coal fields have significantly different contents of As and Se, which offers an opportunity to infer the possible region of coal production. For example, the average As content of coal in northern China (0.4-10 mg kg-1; mg As per kg coal) and southern China (0.5-25 mg kg-1) are 3 mg kg-1 and 10 mg kg-1, respectively (Zhang, 2010; Ren, 2006). With an average value of 2 mg kg-1, the Se content in various Chinese coal fields ranges from 0.1 mg kg-1 to 13 mg kg-1 (Zhang, 2010; Ren, 2006). We have no direct information regarding As and Se contents in coal used in Shanghai. As an alternative, here the average ratio of ambient As and Se (As/Se ratio) in Shanghai was calculated as 2.65, which was very close to the As/Se ratio (2.76) in coal (long flame coal of the Jurassic period) of Henan Province in northern China (Zhang, 2010). Note that the As/Se ratios in Shanxi Province, a major coal production region in China, range from 0.24 in Taiyuan (the capital city of Shanxi) to 1.96 in Datong (a prefecture-level city in northern Shanxi) (Zhang, 2010). The emission source regions of Cu, K, Pb, As, and Se are demonstrated in Fig. 17, in which all species are generally transported from far western Shanghai (where stationary combustion of coal is located; Fig. 1) to our sampling site.

It is well known that Ca and Si are two of the five most abundant elements in the Earth's crust, with a reputation of being the most specific tracers of wind-blown dust. Located on the eastern coast of China, Shanghai rarely receives long-range transport of crustal matters from aeolian dust and the Gobi Desert in northwestern China (Huang et al., 2013). Sampling at the east side of Shanghai, a majority of measured Ca and Si must be sourced from road fugitive dust or urban construction sites, which can be further validated by the CPF and BPP analysis of Ca and Si (Fig. S3). As discussed above, ambient Fe and Ba at PEMC are strongly associated with brake wear (Zhao et al., 2015).

In Fig. 15, significant correlations are observed for Ca, Si, Fe, and Ba, suggesting that the measured Ca and Si during our study period was most likely derived from road fugitive dust.

As a group of tightly-linked metal species, identifying a principle source for measured Cr, Mn and Zn at PEMC is a challenging task. Cr, Mn and Zn have relatively good correlation with two groups of metal species, i.e., coal combustion-related emissions (i.e., Cu, K, Pb, As, and Se) and brake wear-related emissions (i.e., Fe and Ba). This is basically attributed to the diverse sources of Cr, Mn and Zn themselves in China. For Cr, the national atmospheric emissions from anthropogenic sources in 2010 was 7465.2 metric tons, of which 5317.6 metric tons were emitted from coal consumption by industrial boilers (Tian et al., 2015). Coal combustion is also the dominant source of Mn at a national scale, while in urban areas with intensive road network, the contribution of brake and tire wear to ambient Mn is appreciable. In contrast to Cr and Mn, the ferrous metals smelting sector (31.3%), especially the pig iron and steel production industry, is the leading contributor to Zn emissions in China, followed by coal combustion (21.7%) and the nonferrous metals smelting sector (19.3%). The Baosteel company in Shanghai, located to the northwest of PEMC (approximately 20 km apart; Fig. 1), is a flagship manufacturer in terms of producing the first-chop iron and steel throughout China. Fig. S4 also evidently reflects that high concentrations of Zn can occur in the northwest of PEMC. In summary, ambient Cr, Mn and Zn in the Shanghai urban atmosphere is highly mixed with coal combustion by industry sectors and power plants, ferrous metal production, and nonferrous metal smelting.

3.2 Source analysis

In the PMF analysis, three to ten factor solutions were initially examined, from which possible solutions (i.e., four to six factor solutions) were chosen based on the change of Q/Q_{exp}, the achievement of the constant and global minimum of Q, the displacement of factor elements, and the interpretation of physically meaningful factors (Text S1; see discussion below). The most reliable solution was explained by five factors. The chemical profiles and average contributions of the five factors are presented in Fig. 4 with the time-series evolution of these factors included in the Supplement (Fig. S9). On the one hand, we will use various mathematical and physical criteria to constrain different solutions of source apportionment. On the other hand, we will take CPF and BPP as diagnostic tools for quickly gaining the idea of potential source regions, which in turn will contribute to further analysis of source apportionment. Ultimately, the five factors were assigned to different sources, i.e., traffic-related, shipping, nonferrous metal smelting, coal combustion, and ferrous metal smelting.

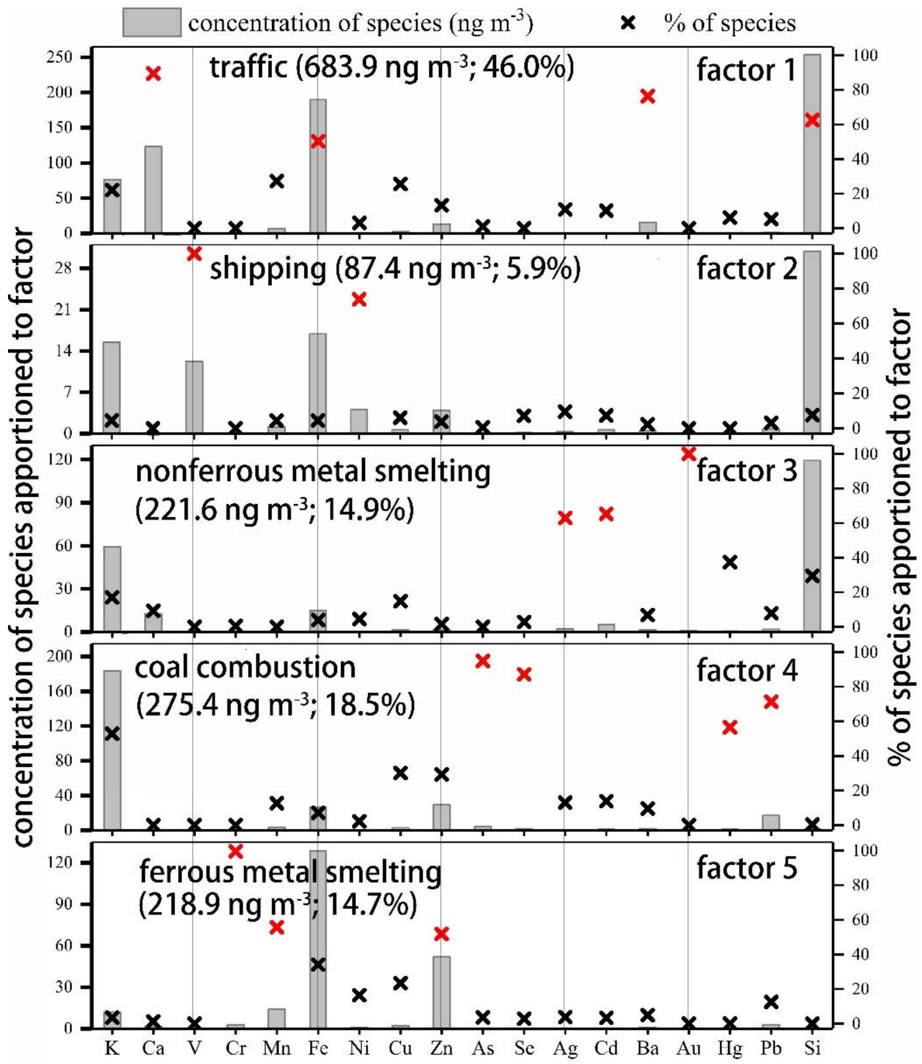

Figure 4. PMF-resolved source profiles (concentration and % of species apportioned to factor) and average contributions (in the parentheses) of individual sources to measured total $PM_{2.5}$ elements in Shanghai. The notable species for each factor/source are marked in red.

3.2.1 Traffic-related

Factor 1 was characterized by a large mass fraction of Ca, Fe, Ba, and Si, which explained 89.5%, 50.3%, 76.5%, and 62.6% of the variation, respectively. This mixed factor is similar to that reported by Amato et al. (2009, 2013), Bukowiecki et al. (2010), Harrison et al. (2012), and Visser et al. (2015b). In urban atmosphere, Fe can be released from engine oil or catalyst equipped gasoline vehicles (Chen et al., 2007). Besides, Fe is linked to non-exhaust emissions such as brake wear because it is the support material for brake pads, and the agents present in brake linings typically consist of Ba, Mn and Cu (Lough et al., 2005; Hjortenkrans et al., 2007; Dall'Osto et al., 2016). Therefore, Fe and Ba can be regarded as chemical tracers for traffic-related source (exhaust and non-exhaust) (Thorpe et al., 2008; Lin et al., 2015). Ca and Si are known as two of the most abundant elements in the upper continental crust, and their atmospheric origins typically attributed to wind-blown dust. Located on the eastern coast of China, Shanghai rarely receives long-range transport of crustal matter from aeolian dust and the Gobi Desert in northwestern China (Huang et al., 2013). Sampling in the urban area of Shanghai, airborne Ca and Si should be dominated by anthropogenic activities like road fugitive dust or urban construction works. In Fig. S10, significant correlations are observed for Ca, Si, Fe, and Ba, suggesting that the measured Ca and Si during our study period were more likely derived from road fugitive dust. Therefore, factor 1 can be assigned to traffic-related source and it was the largest source in Shanghai, accounting for 46.0% (683.9 ng m^{-3}) of the total measured elemental mass in $PM_{2.5}$.

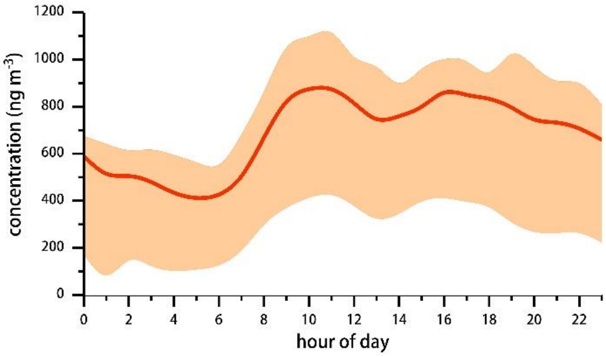

Figure 5. Diurnal variation of PMF-derived elemental concentration for factor 1. The red line, bottom boundary, and upper boundary represent the mean, 1st quartile, and

3rd quartile of the concentration value, respectively.

Hourly measurements over one-year periods provide a unique opportunity to examine the diurnal profile of factor 1. As reported in Fig. 5, the concentration of trace elements contributed by factor 1 shows a marked bimodal diurnal cycle, with average values at rush hours are over two times higher than at nighttime. Such variation pattern agrees well with the diurnal variation of traffic flow in Shanghai (Chang et al., 2016a), further confirming that factor 1 can be interpreted as traffic-related emissions.

3.2.2 Shipping

In Fig. 4, V (100%) and Ni (74%) comes almost exclusively from factor 2, while factor 2 contributes to less than 10% of any other elemental species. V is typically emitted from oil and petrochemical refining and combustion, and natural gas extraction and processing (Duce and Hoffman, 1976; Hope, 1994; Shafer et al., 2012). From CPF and BPP analysis (Fig. S11), higher concentrations of both V and Ni were observed when winds originated from east, northeast, and southeast directions. The most dominant directions were east and southeast, suggesting the influence from costal port cluster or petroleum refinery industry located east/southeast of Shanghai (Fig. 1). Gathering evidence revealed that the ratio of V/Ni can serve as a robust indicator of shipping emissions (Tao et al., 2013; Celo et al., 2015; Liu et al., 2017; Viana et al., 2009). Recent study in Shanghai port suggested that the ratio of V/Ni in aerosols emitted from heavy oil combustion of ocean-going ship engines was 3.4 on average (Zhao et al., 2013). Here measured in urban area, the average ratio of V/Ni in our study was 3.1 with slightly seasonal changes (Fig. 6), indicating V- and Ni-containing aerosols from shipping emissions subject to minor atmospheric transformation. In short, factor 2 likely corresponds to shipping emissions (instead of petrochemical refining), which is consistent with the results of many previous source apportionment works (e.g., Liu et al., 2017; Zhao et al., 2013; Cesari et al., 20014; Healy et al., 2010).

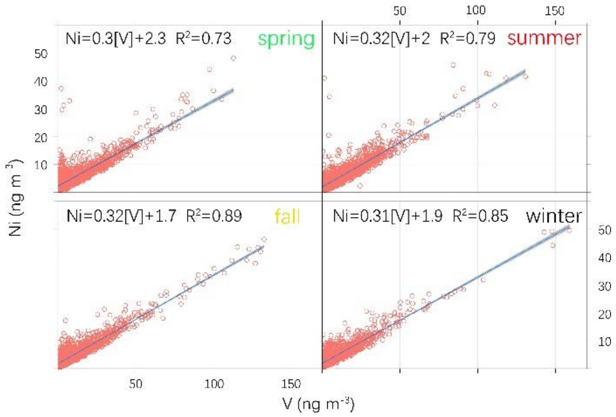

Figure 6. Linear correlation analysis between V (x axis) and Ni (y axis) in Shanghai during four seasons.

Although shipping emissions only contribute to 5.9% of trace elements in Shanghai urban center, its share can be expected to greatly increase in harbor district (Zhao et al., 2013). The good news is that since 1 January 2016, the sea areas of Shanghai and its neighboring ports were designed as shipping emission control area, requiring use of lower sulfur fuels in place of heavy fuel oil in main engines of ships (Zhen et al., 2018). Therefore, it is critically important to assess the impacts of fuel changes on air quality in Shanghai in the future through continuous measurements of trace elements.

3.2.3 Nonferrous metal smelting

The predominant elements found in factor 3 were Au (100%), Cd (65%), and Ag (63%) with 37% of Hg. These four heavy metals are important associated elements in Cu, Pb, and Zn ores. In fact, Cu, Pb, and Zn smelting represent the three most common form of nonferrous metal smelting in China (Tian et al., 2015). Because of high temperatures during roasting, sintering and smelting process for the extraction of Cu, Pb, and Zn from ores, metals like Au, Cd, Ag, and Hg in nonferrous metal ores will inevitably be vaporized and released into the flue gas (Pacyna and Pacyna, 2001; Wu et al., 2012). Therefore, factor 3 was interpreted as nonferrous metal smelting emissions and the contribution of this factor was 14.9% (221.6 ng m^{-3}) to total measured elemental mass in $PM_{2.5}$.

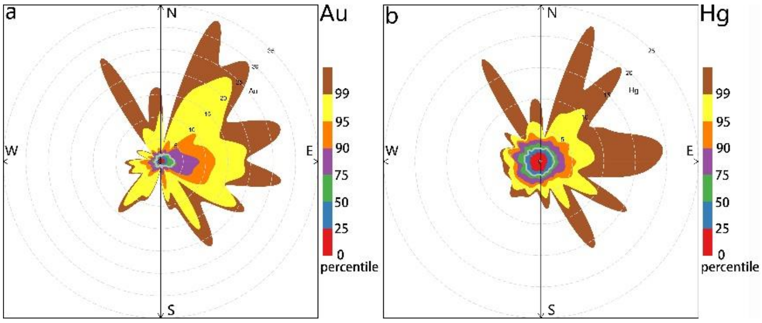

Figure 7. Percentile rose plot of Au (**a**) and Hg (**b**) concentrations in Shanghai between March 2016 and February 2017. The percentile intervals are shaded and shown by wind direction.

To further pinpoint the specific subsector of nonferrous metal smelting, here we calculate percentile concentration levels of Au and Hg, and plot them by wind direction in Fig. 7 (and Ag, Cd in Fig. S12). It clearly shows Au and Hg largely share the same source region that different from Ag and Cd, indicating that Au and Hg were emitted from a similar subsector of nonferrous metal smelting. In Shanghai, Zn smelting is the most important contributor of Hg emissions from the nonferrous metal smelting sector. Therefore, element Au resolved in factor 3 during our study period can be expected to be originated from Zn smelting.

3.2.4 Coal combustion

The most abundant elements found in factor 4 were As, Se, Pb, Hg (explaining 56% to 95% of the variation) with some contributions of Cu (30%), Zn (29%) and unexpected large amount of K (53%). As, Se, Pb, Hg, and Cu are typical marker elements for coal combustion. In China, 73% of As, 62% of Se, 56% of Pb, and 47% of Hg were found to be emitted from coal combustion, and coal consumption in southern China (including Shanghai) is mainly driven by industrial boilers and power plant (Tian et al., 2015). As the largest city-scale coal consumer in China, coal combustion contributed to 275.4 ng m^{-3} or 18.5% of $PM_{2.5}$ trace elements during our study period.

Traditionally, K in particles was considered to be originated from biomass burning along with some contribution of fugitive dust (Zhang et al., 2010; Hueglin et al., 2005;

Fang et al., 2015). Here we show that over half of element K in urban Shanghai were derived from coal combustion. The reason for this discrepancy maybe that in most previous studies, K in particles was pretreated using deionized water to extract (Wang et al., 2013b). In fact, K has high mineral affinity (elements associated with aluminosilicates, carbonates and other minerals in coal ash), and in some extreme cases, only about 1% of K in fly ash from coal combustion can be extracted by water (Querol et al., 1996). For example, particles collected from coal combustion by Wang et al. (2013b) were extracted with deionized water, then atomized and measured by an ATOFMS. The ATOFMS mass spectrum contained relatively low K peak. The observation by Wang et al. (2013) was not consistent with that of Suess et al. (2002), in which they detected larger K peaks in ATOFMS spectra for coal combustion particles in an in situ measurement (i.e. freshly emitted particles were directly introduced into ATOFMS and measured).

3.2.5 Ferrous metal smelting

Factor 5 was distinguished by high levels of Cr, Mn, and Zn representing 100%, 56%, and 52% of the explained variation, respectively. These elements are typically emitted from ferrous metal smelting. For example, the steel production industry represents the dominant contributor to Zn emissions, accounting for about 60% in China (Tian et al., 2015). Driven by rapid modernization of its infrastructure and manufacturing industries, China produced more than 49% of world steel production in 2017 (around 830 million tons), and 6 of 10 of the largest steel producers are in China (data retrieved from https://www.worldsteel.org). Headquartered in Shanghai (20 km northwest of the sampling site), the Baosteel is the fifth-largest steel producer in the world measured by crude steel output, with an annual output of around 35 million tons. Meanwhile, there are several factories of ferrous metal processing located in western Shanghai (Fig. 1). Since element Cr is reported to be transported over distances by air flow (Perry et al., 1999), the presence of ferrous metal smelting activities in the west/northwest of the sampling site is inferred to be associated with this factor based on the results of CPF and BBP in Fig. 8. Overall, ferrous metal smelting contributed 218.9 ng m^{-3} or 14.7%

of $PM_{2.5}$ trace elements in Shanghai.

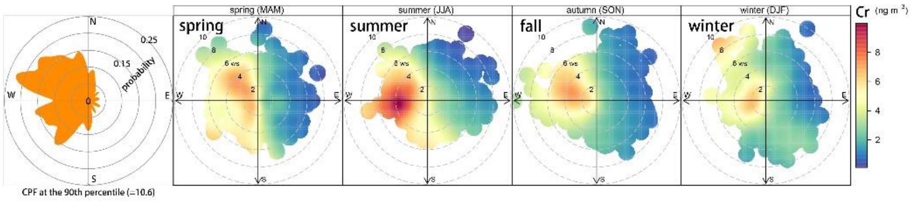

Figure 8. Conditional probability function analysis (left) and bivariate polar plots (right) of seasonal concentrations (in ng m^{-3}) of Cr in Shanghai between March 2016 and February 2017. The center of each plot (centered at the sampling site) represents a wind speed of zero, which increases radially outward. The concentration is shown by the color scale.

5.4 Precipitation effect

Theoretically, precipitation could enhance the wet scavenging of airborne pollutants and reduce their ability to suspend because the increased moisture might capture the particles on the road surface (Kuhns et al., 2003; Karanasiou et al., 2011). Water spray (from sprinkler on road or atop tall building) to simulate natural types of precipitation has been proposed as an important abatement strategy to facilitate the reduction of ambient PM concentrations (including trace elements) in urban China (Liu et al., ,2014; Yu, 2014). However, several field measurements revealed that water spray activities did not influence PM mass levels (e.g., Karanasiou et al., 2012, 2014). Taking advantage of our simultaneous and hourly record of precipitation amount (up to 36.8 mm) and elements concentration, here we evaluate the effects of precipitation on the mitigation of $PM_{2.5}$ trace elements. The precipitation (all were in the form of rainfall) distributed during the full year of measurements is shown in Figure S13. The mass concentrations of trace elements six hours before and after precipitation events were compared from the perspective of individual species and sources. The precipitation event in this study is defined as (1) there are at least six consecutive hours with hourly rainfall amount higher than 1 mm; (2) the consecutive no-rainy time in a precipitation event should less than six hours; (3) the total no-rainy time should less than 1/3 of the entire time of a precipitation event; (4) if the rainfall amount of a specific hour is less than 0.1 mm, and there are at least three no-rainy hours before and after the rainy hour, then this hour should be treated as no-rainy hour. Consequently, 12 precipitation events during our study period were identified with the duration time and accumulated rainfall ranging from 7 to 55 hours, and 26.4 to 217.5 mm, respectively (Table S2).

3.3.1 Change of mass concentration by species

The average mass concentration of each elemental species before, during, and after every precipitation event is presented in Fig. S13. If precipitation effectively scavenge and remove aerosol, then the mass concentrations of trace elements during a precipitation event should lower than that before and after this precipitation event. However, there is no uniform variation pattern in Fig. S14, indicating that precipitation may not be the predominant factor to influence ambient elements mass in some cases. For example, most elemental species had a relatively higher mass concentration during the 12th precipitation event (lasted from 09:00 25 December to 22:00 26 December; Fig. S14). This can be explained by the much less anthropogenic activities during the periods prior to (3:00 to 8:00) and after (23:00 to 3:00 the next day) the 12th precipitation event.

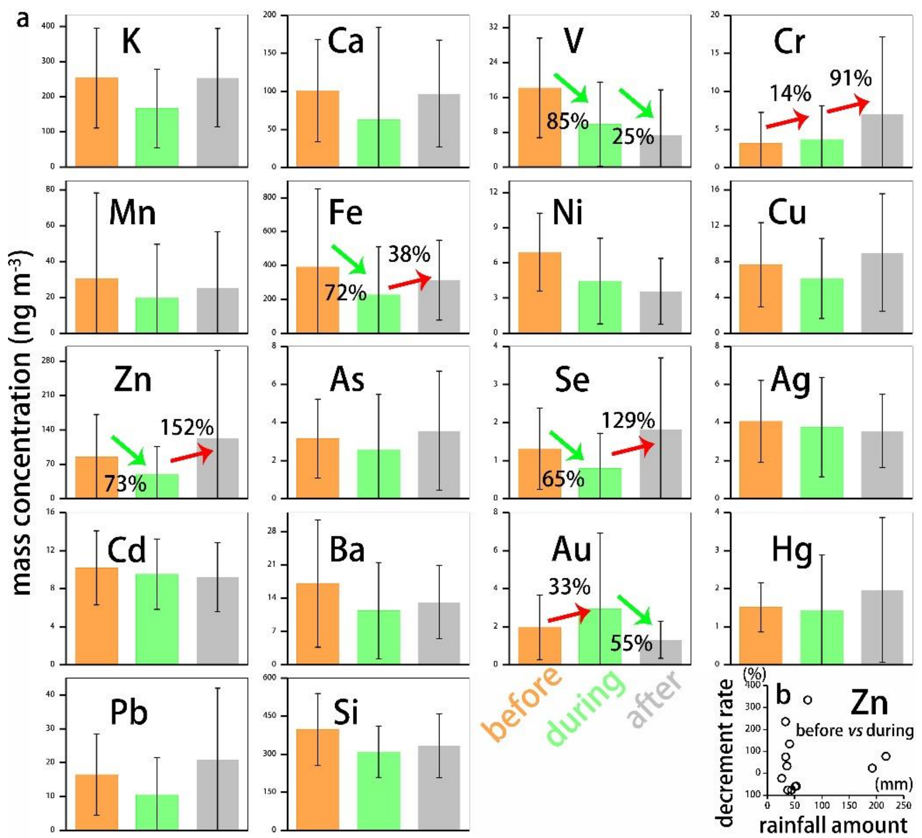

Figure 9. (**a**) The variation of the overall mass concentration of each elemental

species before, during, and after the total 12 precipitation events; (**b**) scatter plot of the relationship between the rainfall amount of each precipitation event and the decrement rate of Zn concentration from the period before precipitation to the period after precipitation.

For each elemental species, the variation of mass concentration before, during, and after every precipitation event were aggregated and reported in Fig. 9a. Before precipitation events, the mass concentrations of all species except Cr and Au were higher than that during precipitation events (notably V, Zn, Fe), suggesting that water spray could generally help to reduce $PM_{2.5}$ trace elements load in the atmosphere. After precipitation events, there were six species (notably V and Au) with their mass concentrations lower than that during precipitation events, indicating potential long-lasting aftereffect of precipitation scavenging. Among all elemental species, the mass concentrations of Zn and Se fluctuate as the most ideal V-shape, which properly reflect the cycle of precipitation. However, as shown in Fig. 9b, a linear relationship cannot be observed between the decrement rate of Zn concentration and rainfall amount of each precipitation event. Although we failed to pinpoint the exact value in this study, our results imply that there is a threshold of precipitation amount to lower ambient $PM_{2.5}$ trace elements mass.

3.3.1 Change of mass concentration by sources

The variation of the overall mass concentration of trace elements contributed by each source and their relative contributions before, during, and after the total 12 precipitation events is shown in Fig. 10a to 10e, and Fig. 10f, respectively. The mass concentration of traffic-related trace elements experienced the sharpest decrease during the transition of no-rainy hours to rainy hours (159%), and a moderate rebound after precipitation (35%). Fang et al. (2015) found that mobile source emissions generated through mechanical processes (re-entrained road dust, tire and break wear) and processing by secondary sulfate were major contributors to water-soluble metals. In our study, traffic-related source mainly includes road dust and brake wear, which can not only be easily removed through precipitation but also can hardly be blown up from wet road surface after raining. In comparison, the mass contribution of coal combustion source was also wet removed rapidly first (139%) due to its tracer elements like As, Se, Pb, and Hg have larger water-soluble fraction. However, after precipitation, the contribution of coal combustion source dramatically increased over two times (Fig. 10d and 10f). This can be explained that different from traffic-related source, coal combustion-related trace elements are generally emitted through elevated chimneys in the sectors of industrial broilers and power plants. The mass concentrations of trace elements contributed by nonferrous and ferrous metal smelting during the three periods kept quite flat (Fig. 10c and 10d), suggesting that precipitation has little effect on ambient trace elements emitted from metal smelting activities. Nevertheless, given that traffic-related and coal combustion are the dominant contributors to ambient $PM_{2.5}$ trace elements, our results validate that water spray could be an effective approach to help curb the severe atmospheric metal pollution in many Chinese cities.

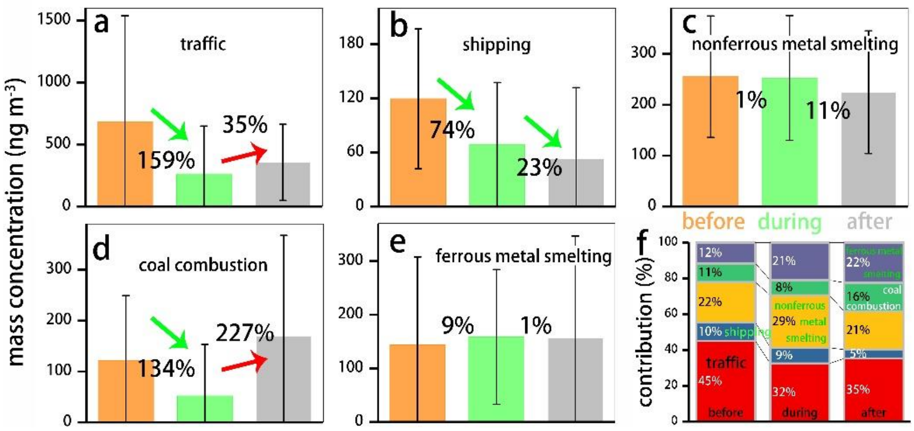

Figure 10. The variation of the overall mass concentration of trace elements contributed by traffic-related (**a**), shipping (**b**), nonferrous metal smelting (**c**), coal combustion (**d**), and ferrous metal smelting (**e**), and their relative contributions (**f**) before, during, and after the total 12 precipitation events.

In Fig. 10b and 10f, the contribution of shipping emissions to ambient trace elements (mainly V and Ni) during the three periods reduced continuously. Mostly transported from Eastern China sea, V and Ni almost exclusively originated from the east of the sampling site. In other words, the contribution of shipping emissions to urban atmosphere is supposed to be very sensitive to wind speed and wind direction in Shanghai. The wind roses for the three periods are presented in Fig. 11. It shows that before precipitation events, the average wind speed (± 1σ) was the lowest (2.3 ± 1.3 m s^{-1}), and easterly winds prevail in most times. These factors are favorable to the transportation of shipping emissions from Eastern China sea and then accumulated in Shanghai urban atmosphere. In contrast to the period before precipitation events, the average wind speed after precipitation events was the highest (3.1 ± 2.1 m s^{-1}) with northwesterly and northerly winds from mainland China can dilute shipping-related trace elements to the lowest levels (Fig. 10b). In brief, the mass concentration of shipping-related trace elements in Shanghai urban atmosphere is more likely to be influenced by winds instead of precipitation.

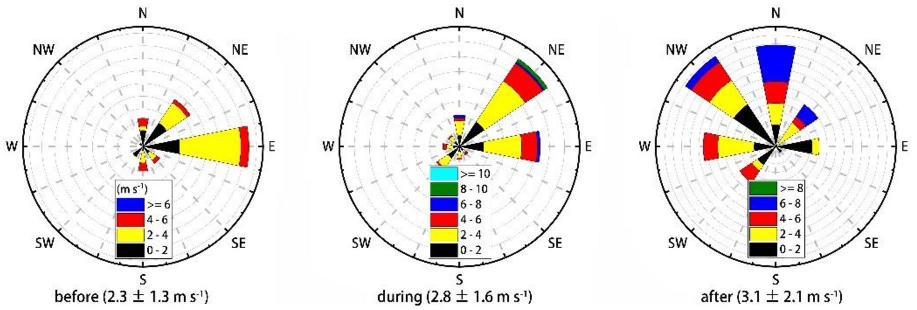

Figure 11. Wind roses plots for the periods before, during, and after the twelve precipitation events. The average wind speed (± 1σ) for each period is shown in bracket.

4. Conclusion and outlook

This paper presents the results from a year-long, near real-time measurement study of 18 trace elements (Si, Fe, K, Ca, Zn, Mn, Pb, Ba, V, Cu, Cd, As, Ni, Cr, Ag, Se, Hg, and Au) in $PM_{2.5}$ using a Xact multi-metal monitor, conducted at an urban site in Shanghai from March 2016 to February 2017. The scientific significance of this work can be reflected by the general findings as follows:

-The Xact multi-metals monitor was demonstrated as a valuable and practical tool for ambient monitoring of atmospheric trace elements by comparing online monitoring results with ICP analyses of offline filter samples.

-The metal concentrations in Shanghai are one or two orders of magnitude higher than in north America and Europe, highlighting the need to allocate more scientific, technical, and legal resources on controlling metal emissions in China.

-The total of metal related species comprised approximately 8.3% of the $PM_{2.5}$ mass, which should not be ignored in China's recent epidemiologic study of attributing hospital emergency-room visits to $PM_{2.5}$ chemical constituents.

-The full coverage of trace elemental species (18) measurement and the high temporal frequency (hourly) in the work provided unprecedented details regarding the temporal evolution of metal pollution and its potential sources in Shanghai.

-Five sources, i.e., traffic-related, shipping, nonferrous metal melting, coal combustion, and ferrous metal smelting were identified by PMF analysis, which contributed to 46%, 6%, 15%, 18%, and 15% of ambient $PM_{2.5}$ trace elements, respectively.

-The dominant contributors of trace elements (traffic-related and coal combustion) can be effectively removed through precipitation from the atmosphere, suggesting that water spray can be used to curb $PM_{2.5}$ trace elements in urban atmosphere.

A greater value and more interesting topic to the scientific community would be to fully assess the role of $PM_{2.5}$ chemical constituents (including metal species) and sources of emission to human health. Looking towards the future, three major steps will be taken toward thoroughly addressing these questions. Firstly, characterizing the chemical and isotopic (including metal species) signatures of emission sources will be intensively undertaken through field sampling as well as for laboratory simulations (see example of Geagea et al. (2007)). Secondly, the Xact multi-metals monitor, Sunset OC/EC analyzer (Chang et al., 2017), and MARGA (Monitoring of AeRosols and Gases) platform will be collocated across a rural-urban-background transect to simultaneously measure hourly metal species, carbonaceous aerosols, and inorganic aerosol components in $PM_{2.5}$. Lastly, integrating all available information regarding $PM_{2.5}$ chemical species and isotopes into a receptor model or atmospheric chemical transport model will be carried forward to create more specific and confident source apportionment results.

Competing interests

The authors declare that they have no competing interests.

Data availability

Data are available from the corresponding authors on request.

Acknowledgements

This study was supported by the National Key Research and Development Program of China (2017YFC0212700), National Natural Science Foundation of China (Grant nos. 41705100, 91644103, 41603104, 41429501, and 91644105), Provincial Natural Science Foundation of Jiangsu (BK20170946), University Science Research Project of Jiangsu Province (17KJB170011), and the Priority Academic Program Development of Jiangsu Higher Education Institutions (PAPD). Many thanks go to Tony Dore at the Centre for Ecology and Hydrology, Edinburgh, United Kingdom for his linguistic corrections.

Reference

Amato, F., Pandolfi, M., Escrig, A., Querol, X., Alastuey, A., Pey, J., Perez, N., and Hopke, P. K.: Quantifying road dust resuspension in urban environment by Multilinear Engine: A comparison with PMF2, Atmos. Environ., 43, 2770-2780, doi: 10.1016/j.atmosenv.2009.02.039, 2009.

Amato, F., Pandolfi, M., Moreno, T., Furger, M., Pey, J., Alastuey, A., Bukowiecki, N., Prevot, A. S. H., Baltensperger, U., and Querol, X.: Sources and variability of inhalable road dust particles in three European cities, Atmos. Environ., 45, 6777-6787, doi: 10.1016/j.atmosenv.2011.06.003, 2011.

Amato, F., Schaap, M., Denier van der Gon, H. A. C., Pandolfi, M., Alastuey, A., Keuken, M., and Querol, X.: Short-term variability of mineral dust, metals and carbon emission from road dust resuspension, Atmos. Environ., 74, 134-140, doi: 10.1016/j.atmosenv.2013.03.037, 2013.

Brandt, C. and van Eldik, R.: Transition metal-catalyzed oxidation of sulfur (IV) oxides. Atmospheric-relevant processes and mechanisms, Chem. Rev., 95, 119-190, doi: 10.1021/cr00033a006, 1995.

Bukowiecki, N., Hill, M., Gehrig, R., Zwicky, C. N., Lienemann, P., Hegedüs, F., Falkenberg, G., Weingartner, E., and Baltensperger, U.: Trace metals in ambient air: Hourly size-segregated mass concentrations determined by synchrotron-XRF, Environ. Sci. Technol., 39, 5754-5762, doi: 10.1021/es048089m, 2005.

Bukowiecki, N., Lienemann, P., Hill, M., Furger, M., Richard, A., Amato, F., Prévôt, A. S. H., Baltensperger, U., Buchmann, B., and Gehrig, R.: PM_{10} emission factors for

non-exhaust particles generated by road traffic in an urban street canyon and along a freeway in Switzerland, Atmos. Environ., 44, 2330-2340, doi: 10.1016/j.atmosenv.2010.03.039, 2010.
Burnett, R. T., Pope, C. A., III, Ezzati, M., Olives, C., Lim, S. S., Mehta, S., Shin, H. H., Singh, G., Hubbell, B., Brauer, M., Anderson, H. R., Smith, K. R., Balmes, J. R., Bruce, N. G., Kan, H., Laden, F., Pruss-Ustun, A., Turner, M. C., Gapstur, S. M., Diver, W. R., and Cohen, A.: An integrated risk function for estimating the global burden of disease attributable to ambient fine particulate matter exposure, Environ. Health. Perspect., 122, 397-403, doi: 10.1289/ehp.1307049, 2014.
Carslaw, D. C., Beevers, S. D., Ropkins, K., and Bell, M. C.: Detecting and quantifying aircraft and other on-airport contributions to ambient nitrogen oxides in the vicinity of a large international airport, Atmos. Environ., 40, 5424-5434, doi: 10.1016/j.atmosenv.2006.04.062, 2006.
Carslaw, D. C. and Ropkins, K.: Openair - An R package for air quality data analysis, Environ. Modell. Softw., 27–28, 52-61, doi: 10.1016/j.envsoft.2011.09.008, 2012.
Cate, D. M., Noblitt, S. D., Volckens, J., and Henry, C. S.: Multiplexed paper analytical device for quantification of metals using distance-based detection, Lab Chip, 15, 2808-2818, doi: 10.1039/c5lc00364d, 2015.
Celo, V., Dabek-Zlotorzynska, E., and McCurdy, M.: Chemical characterization of exhaust emissions from selected Canadian marine vessels: the case of trace metals and lanthanoids, Environ. Sci. Technol., 49, 5220-5226, doi: 10.1021/acs.est.5b00127, 2015.
Cesari, D., Genga, A., Ielpo, P., Siciliano, M., Mascolo, G., Grasso, F. M., and Contini, D.: Source apportionment of $PM_{2.5}$ in the harbour–industrial area of Brindisi (Italy): Identification and estimation of the contribution of in-port ship emissions, Sci. Total Environ., 497-498, 392-400, doi: 10.1016/j.scitotenv.2014.08.007, 2014.
Chang, Y., Zou, Z., Deng, C., Huang, K., Collett, J. L., Lin, J., and Zhuang, G.: The importance of vehicle emissions as a source of atmospheric ammonia in the megacity of Shanghai, Atmos. Chem. Phys., 16, 3577-3594, doi: 10.5194/acp-16-3577-2016, 2016.
Chang, Y., Deng, C., Cao, F., Cao, C., Zou, Z., Liu, S., Lee, X., Li, J., Zhang, G., and Zhang, Y.: Assessment of carbonaceous aerosols in Shanghai, China: Long-term evolution, seasonal variations and meteorological effects, Atmos. Chem. Phys. Discuss., 2017, 1-46, doi: 10.5194/acp-2017-50, 2017.
Charrier, J. G. and Anastasio, C.: On dithiothreitol (DTT) as a measure of oxidative potential for ambient particles: evidence for the importance of soluble transition metals, Atmos. Chem. Phys., 12, 9321-9333, doi: 10.5194/acp-12-9321-2012, 2012.
Chen, B., Stein, A. F., Castell, N., Gonzalez-Castanedo, Y., Sanchez de la Campa, A. M., and de la Rosa, J. D.: Modeling and evaluation of urban pollution events of atmospheric heavy metals from a large Cu-smelter, Sci. Total Environ., 539, 17-25, doi: 10.1016/j.scitotenv.2015.08.117, 2016.
Chen, L. W. A., Watson, J. G., Chow, J. C., and Magliano, K. L.: Quantifying $PM_{2.5}$ source contributions for the San Joaquin Valley with multivariate receptor models,

Environ. Sci. Technol., 41, 2818-2826, doi: 10.1021/es0525105, 2007.
Cooper, J. A., Petterson, K., Geiger, A., Siemers, A., and Rupprecht, B.: Guide for developing a multi-metals, fenceline monitoring plan for fugitive emissions using X-ray based monitors, Cooper Environmental Services, Portland, Oregon, 1-42, 2010.
Dabek-Zlotorzynska, E., Dann, T. F., Kalyani Martinelango, P., Celo, V., Brook, J. R., Mathieu, D., Ding, L., and Austin, C. C.: Canadian National Air Pollution Surveillance (NAPS) $PM_{2.5}$ speciation program: Methodology and $PM_{2.5}$ chemical composition for the years 2003–2008, Atmos. Environ., 45, 673-686, doi: 10.1016/j.atmosenv.2010.10.024, 2011.
Dall'Osto, M., Beddows, D. C. S., Harrison, R. M., and Onat, B.: Fine iron aerosols are internally mixed with nitrate in the urban European atmosphere, Environ. Sci. Technol., 50, 4212-4220, doi: 10.1021/acs.est.6b01127, 2016.
Dall'Osto, M., Querol, X., Amato, F., Karanasiou, A., Lucarelli, F., Nava, S., Calzolai, G., and Chiari, M.: Hourly elemental concentrations in $PM_{2.5}$ aerosols sampled simultaneously at urban background and road site during SAPUSS - diurnal variations and PMF receptor modelling, Atmos. Chem. Phys., 13, 4375-4392, doi: 10.5194/acp-13-4375-2013, 2013.
DeCarlo, P. F., Kimmel, J. R., Trimborn, A., Northway, M. J., Jayne, J. T., Aiken, A. C., Gonin, M., Fuhrer, K., Horvath, T., Docherty, K. S., Worsnop, D. R., and Jimenez, J. L.: Field-deployable, high-resolution, time-of-flight aerosol mass spectrometer, Anal. Chem., 78, 8281-8289, doi: 10.1021/ac061249n, 2006.
Duan, J. and Tan, J.: Atmospheric heavy metals and arsenic in China: Situation, sources and control policies, Atmos. Environ., 74, 93-101, doi: 10.1016/j.atmosenv.2013.03.031, 2013.
Duce, R. A., and Hoffman, G. L.: Atmospheric vanadium transport to the ocean, Atmos. Environ., 10, 989-996, doi: 10.1016/0004-6981(76)90207-9, 1976.
Fan, Q., Zhang, Y., Ma, W., Ma, H., Feng, J., Yu, Q., Yang, X., Ng, S. K. W., Fu, Q., and Chen, L.: Spatial and seasonal dynamics of ship emissions over the Yangtze River Delta and East China Sea and their potential environmental influence, Environ. Sci. Technol., 50, 1322-1329, doi: 10.1021/acs.est.5b03965, 2016.
Fang, T., Guo, H., Verma, V., Peltier, R. E., and Weber, R. J.: $PM_{2.5}$ water-soluble elements in the southeastern United States: Automated analytical method development, spatiotemporal distributions, source apportionment, and implications for heath studies, Atmos. Chem. Phys., 15, 11667-11682, doi: 10.5194/acp-15-11667-2015, 2015.
Fergusson, J. E.: The heavy elements: Chemistry, environmental impact and health effects, Pergamon Press, Oxford, UK, pp 614, 1990.
Furger, M., Minguillón, M. C., Yadav, V., Slowik, J. G., Hüglin, C., Fröhlich, R., Petterson, K., Baltensperger, U., and Prévôt, A. S. H.: Elemental composition of ambient aerosols measured with high temporal resolution using an online XRF spectrometer, Atmos. Meas. Tech., 10, 2061-2076, doi: 10.5194/amt-10-2061-2017, 2017.
Geagea, M. L., Stille, P., Millet, M., and Perrone, T.: REE characteristics and Pb, Sr and

Nd isotopic compositions of steel plant emissions, Sci. Total Environ., 373, 404-419, doi: 10.1016/j.scitotenv.2006.11.011, 2007.
Gross, D. S., Gälli, M. E., Silva, P. J., and Prather, K. A.: Relative sensitivity factors for alkali metal and ammonium cations in single-particle aerosol time-of-flight mass spectra, Anal. Chem., 72, 416-422, doi: 10.1021/ac990434g, 2000.
Han, T., Qiao, L., Zhou, M., Qu, Y., Du, J., Liu, X., Lou, S., Chen, C., Wang, H., Zhang, F., Yu, Q., and Wu, Q.: Chemical and optical properties of aerosols and their interrelationship in winter in the megacity Shanghai of China, J. Environ. Sci. (China), 27, 59-69, doi: 10.1016/j.jes.2014.04.018, 2015.
Harrison, R. M., Jones, A. M., Gietl, J., Yin, J., and Green, D. C.: Estimation of the contributions of brake dust, tire wear, and resuspension to nonexhaust traffic particles derived from atmospheric measurements, Environ. Sci. Technol., 46, 6523-6529, doi: 10.1021/es300894r, 2012.
Healy, R. M., Hellebust, S., Kourtchev, I., Allanic, A., O'Connor, I. P., Bell, J. M., Healy, D. A., Sodeau, J. R., and Wenger, J. C.: Source apportionment of $PM_{2.5}$ in Cork Harbour, Ireland using a combination of single particle mass spectrometry and quantitative semi-continuous measurements, Atmos. Chem. Phys., 10, 9593-9613, doi: 10.5194/acp-10-9593-2010, 2010.
Holden, P. A., Gardea-Torresdey, J. L., Klaessig, F., Turco, R. F., Mortimer, M., Hund-Rinke, K., Cohen Hubal, E. A., Avery, D., Barceló, D., Behra, R., Cohen, Y., Deydier-Stephan, L., Ferguson, P. L., Fernandes, T. F., Herr Harthorn, B., Henderson, W. M., Hoke, R. A., Hristozov, D., Johnston, J. M., Kane, A. B., Kapustka, L., Keller, A. A., Lenihan, H. S., Lovell, W., Murphy, C. J., Nisbet, R. M., Petersen, E. J., Salinas, E. R., Scheringer, M., Sharma, M., Speed, D. E., Sultan, Y., Westerhoff, P., White, J. C., Wiesner, M. R., Wong, E. M., Xing, B., Steele Horan, M., Godwin, H. A., and Nel, A. E.: Considerations of environmentally relevant test conditions for improved evaluation of ecological hazards of engineered nanomaterials, Environ. Sci. Technol., 50, 6124-6145, doi: 10.1021/acs.est.6b00608, 2016.
Honda, T., Eliot, M. N., Eaton, C. B., Whitsel, E., Stewart, J. D., Mu, L., Suh, H., Szpiro, A., Kaufman, J. D., Vedal, S., and Wellenius, G. A.: Long-term exposure to residential ambient fine and coarse particulate matter and incident hypertension in post-menopausal women, Environ. Int., 105, 79-85, doi: 10.1016/j.envint.2017.05.009, 2017.
Hueglin, C., Gehrig, R., Baltensperger, U., Gysel, M., Monn, C., and Vonmont, H.: Chemical characterisation of $PM_{2.5}$, PM_{10} and coarse particles at urban, near-city and rural sites in Switzerland, Atmos. Environ., 39, 637-651, doi: 10.1016/j.atmosenv.2004.10.027, 2005.
Hu, X., Zhang, Y., Ding, Z., Wang, T., Lian, H., Sun, Y., and Wu, J.: Bioaccessibility and health risk of arsenic and heavy metals (Cd, Co, Cr, Cu, Ni, Pb, Zn and Mn) in TSP and $PM_{2.5}$ in Nanjing, China, Atmos. Environ., 57, 146-152, doi: 10.1016/j.atmosenv.2012.04.056, 2012.
Huang, C., Chen, C. H., Li, L., Cheng, Z., Wang, H. L., Huang, H. Y., Streets, D. G., Wang, Y. J., Zhang, G. F., and Chen, Y. R.: Emission inventory of anthropogenic

air pollutants and VOC species in the Yangtze River Delta region, China, Atmos. Chem. Phys., 11, 4105-4120, DOI 10.5194/acp-11-4105-2011, 2011.

Huang, K., Zhuang, G., Lin, Y., Wang, Q., Fu, J. S., Fu, Q., Liu, T., and Deng, C.: How to improve the air quality over megacities in China: Pollution characterization and source analysis in Shanghai before, during, and after the 2010 World Expo, Atmos. Chem. Phys., 13, 5927-5942, doi: 10.5194/acp-13-5927-2013, 2013.

Huang, W., Cao, J., Tao, Y., Dai, L., Lu, S.-E., Hou, B., Wang, Z., and Zhu, T.: Seasonal variation of chemical species associated with short-term mortality effects of $PM_{2.5}$ in Xi'an, a central city in China, Am. J. Epidemiol., 175, 556-566, doi: 10.1093/aje/kwr342, 2012.

Hope, B. K.: A global biogeochemical budget for vanadium, Sci. Total Environ., 141, 1-10, doi: 10.1016/0048-9697(94)90012-4, 1994.

Iyengar, V. and Woittiez, J.: Trace elements in human clinical specimens: evaluation of literature data to identify reference values, Clin. Chem., 34, 474-481, 1988.

Jeong, C. H., Wang, J. M., and Evans, G. J.: Source apportionment of urban particulate matter using hourly resolved trace metals, organics, and inorganic aerosol components, Atmos. Chem. Phys. Discuss., 1-32, doi: 10.5194/acp-2016-189, 2016.

John, D. H.: "Heavy metals"-a meaningless term?, Pure Appl. Chem., 74, 793-807, doi: 10.1351/pac200274050793, 2002.

Jomova, K. and Valko, M.: Advances in metal-induced oxidative stress and human disease, Toxicol., 283, 65-87, doi: 10.1016/j.tox.2011.03.001, 2011.

Karanasiou, A., Moreno, T., Amato, F., Lumbreras, J., Narros, A., Borge, R., Tobías, A., Boldo, E., Linares, C., Pey, J., Reche, C., Alastuey, A., and Querol, X.: Road dust contribution to PM levels – Evaluation of the effectiveness of street washing activities by means of Positive Matrix Factorization, Atmos. Environ., 45, 2193-2201, doi: 10.1016/j.atmosenv.2011.01.067, 2011.

Karanasiou, A., Moreno, T., Amato, F., Tobías, A., Boldo, E., Linares, C., Lumbreras, J., Borge, R., Alastuey, A., and Querol, X.: Variation of $PM_{2.5}$ concentrations in relation to street washing activities, Atmos. Environ., 54, 465-469, doi: 10.1016/j.atmosenv.2012.02.006, 2012.

Karanasiou, A.: Road dust emission sources and assessment of street washing effect, Aerosol Air Qual. Res., doi: 10.4209/aaqr.2013.03.0074, 2014.

Kastury, F., Smith, E., and Juhasz, A. L.: A critical review of approaches and limitations of inhalation bioavailability and bioaccessibility of metal(loid)s from ambient particulate matter or dust, Sci. Total Environ., 574, 1054-1074, doi: 10.1016/j.scitotenv.2016.09.056, 2017.

Khalaf, F., Literathy, P., and Anderlini, V.: Vanadium as a tracer of oil pollution in the sediments of Kuwait, sediment/freshwater interaction, Dordrecht, 1982, 147-154.

Kim, K. H., Kabir, E., and Jahan, S. A.: A review on the distribution of Hg in the environment and its human health impacts, J. Hazard. Mater., 306, 376-385, doi: 10.1016/j.jhazmat.2015.11.031, 2016.

Kloog, I., Ridgway, B., Koutrakis, P., Coull, B. A., and Schwartz, J. D.: Long- and short-term exposure to $PM_{2.5}$ and mortality: Using novel exposure models,

Epidemiol., 24, 555-561, doi: 10.1097/EDE.0b013e318294beaa, 2013.
Kuhns, H., Etyemezian, V., Green, M., Hendrickson, K., McGown, M., Barton, K., and Pitchford, M.: Vehicle-based road dust emission measurement-Part II: Effect of precipitation, wintertime road sanding, and street sweepers on inferred PM_{10} emission potentials from paved and unpaved roads, Atmos. Environ., 37, 4573-4582, doi: 10.1016/S1352-2310(03)00529-6, 2003.
Leung, A. O. W., Duzgoren-Aydin, N. S., Cheung, K. C., and Wong, M. H.: Heavy metals concentrations of surface dust from e-waste recycling and its human health implications in Southeast China, Environ. Sci. Technol., 42, 2674-2680, doi: 10.1021/es071873x, 2008.
Li, H., Wang, J., Wang, Q., Tian, C., Qian, X., and Leng, X.: Magnetic properties as a proxy for predicting fine-particle-bound heavy metals in a support vector machine approach, Environ. Sci. Technol., Environ. Sci. Technol., 51, 6927-6935, doi: 10.1021/acs.est.7b00729, 2017.
Lin, Y. C., Tsai, C. J., Wu, Y. C., Zhang, R., Chi, K. H., Huang, Y. T., Lin, S. H., and Hsu, S. C.: Characteristics of trace metals in traffic-derived particles in Hsuehshan Tunnel, Taiwan: size distribution, potential source, and fingerprinting metal ratio, Atmos. Chem. Phys., 15, 4117-4130, doi: 10.5194/acp-15-4117-2015, 2015.
Litter, M. I.: Heterogeneous photocatalysis: Transition metal ions in photocatalytic systems, Appl. Catal. B: Environ., 23, 89-114, doi: 10.1016/S0926-3373(99)00069-7, 1999.
Liu, Z., Hu, B., Wang, L., Wu, F., Gao, W., and Wang, Y.: Seasonal and diurnal variation in particulate matter (PM_{10} and $PM_{2.5}$) at an urban site of Beijing: Analyses from a 9-year study, Environ. Sci. Pollut. Res. Int., 22, 627-642, doi: 10.1007/s11356-014-3347-0, 2015.
Liu, Z., Lu, X., Feng, J., Fan, Q., Zhang, Y., and Yang, X.: Influence of ship emissions on urban air quality: A comprehensive study using highly time-resolved online measurements and numerical simulation in Shanghai, Environ. Sci. Technol., 51, 202-211, doi: 10.1021/acs.est.6b03834, 2017.
Liu, S., Triantis, K., and Zhang, L.: The design of an urban roadside automatic sprinkling system: mitigation of $PM_{2.5-10}$ in ambient air in megacities, Chinese J. Engineering, 12, doi: 10.1155/2014/618109, 2014.
Lu, S., Yao, Z., Chen, X., Wu, M., Sheng, G., Fu, J., and Paul, D.: The relationship between physicochemical characterization and the potential toxicity of fine particulates ($PM_{2.5}$) in Shanghai atmosphere, Atmos. Environ., 42, 7205-7214, doi: 10.1016/j.atmosenv.2008.07.030, 2008.
Lough, G. C., Schauer, J. J., Park, J. S., Shafer, M. M., DeMinter, J. T., and Weinstein, J. P.: Emissions of metals associated with motor vehicle roadways, Environ. Sci. Technol., 39, 826-836, doi: 10.1021/es048715f, 2005.
Maenhaut, W.: Present role of PIXE in atmospheric aerosol research, Nucl. Instrum. Meth. B, 363, 86-91, doi: 10.1016/j.nimb.2015.07.043, 2015.
Morman, S. A. and Plumlee, G. S.: The role of airborne mineral dusts in human disease, Aeolian Res., 9, 203-212, doi: 10.1016/j.aeolia.2012.12.001, 2013.
Murphy, D. M., Thomson, D. S., and Mahoney, M. J.: In situ measurements of organics,

meteoritic material, mercury, and other elements in aerosols at 5 to 19 kilometers, Science, 282, 1664-1669, doi: 10.1126/science.282.5394.1664, 1998.

Normile, D.: China's living laboratory in urbanization, Science, 319, 740-743, doi: 10.1126/science.319.5864.740, 2008.

Olujimi, O. O., Oputu, O., Fatoki, O., Opatoyinbo, O. E., Aroyewun, O. A., and Baruani, J.: Heavy metals speciation and human health risk assessment at an illegal gold mining site in Igun, Osun State, Nigeria, J. Heal. Pollut., 5, 19-32, doi: 10.5696/i2156-9614-5-8.19, 2015.

Pacyna, J. M. and Pacyna, E. G.: An assessment of global and regional emissions of trace metals to the atmosphere from anthropogenic sources worldwide, Environ. Rev., 9, 269-298, doi: 10.1139/a01-012, 2001.

Pardo, M., Shafer, M. M., Rudich, A., Schauer, J. J., and Rudich, Y.: Single exposure to near roadway particulate matter leads to confined inflammatory and defense responses: Possible role of metals, Environ. Sci. Technol., 49, 8777-8785, doi: 10.1021/acs.est.5b01449, 2015.

Park, S. S., Cho, S. Y., Jo, M. R., Gong, B. J., Park, J. S., and Lee, S. J.: Field evaluation of a near-real time elemental monitor and identification of element sources observed at an air monitoring supersite in Korea, Atmos. Pollut. Res., 5, 119-128, doi: 10.5094/apr.2014.015, 2014.

Perry, K. D., Cahill, T. A., Schnell, R. C., and Harris, J. M.: Long-range transport of anthropogenic aerosols to the National Oceanic and Atmospheric Administration baseline station at Mauna Loa Observatory, Hawaii, J. Geophys. Res., 104, 18521-18533, doi: 10.1029/1998JD100083, 1999.

Phillips-Smith, C., Jeong, C. H., Healy, R. M., Dabek-Zlotorzynska, E., Celo, V., Brook, J. R., and Evans, G.: Sources of particulate matter in the Athabasca oil sands region: Investigation through a comparison of trace element measurement methodologies, Atmos. Chem. Phys. Discuss., 2017, 1-34, doi: 10.5194/acp-2016-966, 2017.

Pope III, C. A., Burnett, R. T., Thun, M. J., Calle, E. E., Krewski, D., Ito, K., and Thurston, G. D.: Lung cancer, cardiopulmonary mortality, and long-term exposure to fine particulate air pollution, J. Am. Med. Assoc., 1132-1141, 2002.

Pope III, C. A., Ezzati, M., and Dockery, D. W.: Fine-particulate air pollution and life expectancy in the United States, New Engl. J. Med., 360, 376-386, doi: 10.1056/NEJMsa0805646, 2009.

Qiao, L., Cai, J., Wang, H., Wang, W., Zhou, M., Lou, S., Chen, R., Dai, H., Chen, C., and Kan, H.: $PM_{2.5}$ constituents and hospital emergency-room visits in Shanghai, China, Environ. Sci. Technol., 48, 10406-10414, doi: 10.1021/es501305k, 2014.

Querol, X., Juan, R., Lopez-Soler, A., Fernandez-Turiel, J., and Ruiz, C. R.: Mobility of trace elements from coal and combustion wastes, Fuel, 75, 821-838, doi: 10.1016/0016-2361(96)00027-0, 1996.

Richard, A., Bukowiecki, N., Lienemann, P., Furger, M., Fierz, M., Minguillón, M. C., Weideli, B., Figi, R., Flechsig, U., Appel, K., Prévôt, A. S. H., and Baltensperger, U.: Quantitative sampling and analysis of trace elements in atmospheric aerosols: impactor characterization and Synchrotron-XRF mass calibration, Atmos. Meas. Tech., 3, 1473-1485, doi: 10.5194/amt-3-1473-2010, 2010.

Ridley, D. A., Heald, C. L., Kok, J. F., and Zhao, C.: An observationally constrained estimate of global dust aerosol optical depth, Atmos. Chem. Phys., 16, 15097-15117, doi: 10.5194/acp-16-15097-2016, 2016.

Rubasinghege, G., Elzey, S., Baltrusaitis, J., Jayaweera, P. M., and Grassian, V. H.: Reactions on atmospheric dust particles: Surface photochemistry and size-dependent nanoscale redox chemistry, J. Phys. Chem. Let., 1, 1729-1737, doi: 10.1021/jz100371d, 2010a.

Rubasinghege, G., Lentz, R. W., Scherer, M. M., and Grassian, V. H.: Simulated atmospheric processing of iron oxyhydroxide minerals at low pH: Roles of particle size and acid anion in iron dissolution, P. Natl. Acad. Sci., 107, 6628-6633, doi: 10.1073/pnas.0910809107, 2010b.

Saffari, A., Daher, N., Shafer, M. M., Schauer, J. J., and Sioutas, C.: Global perspective on the oxidative potential of airborne particulate matter: A synthesis of research findings, Environ. Sci. Technol., 48, 7576-7583, doi: 10.1021/es500937x, 2014.

Seigneur, C. and Constantinou, E.: Chemical kinetic mechanism for atmospheric chromium, Environ. Sci. Technol., 29, 222-231, doi: 10.1021/es00001a029, 1995.

Shafer, M. M., Toner, B. M., Overdier, J. T., Schauer, J. J., Fakra, S. C., Hu, S., Herner, J. D., and Ayala, A.: Chemical speciation of vanadium in particulate matter emitted from diesel vehicles and urban atmospheric aerosols, Environ. Sci. Technol., 46, 189-195, doi: 10.1021/es200463c, 2012.

Shah, A. S. V., Langrish, J. P., Nair, H., McAllister, D. A., Hunter, A. L., Donaldson, K., Newby, D. E., and Mills, N. L.: Global association of air pollution and heart failure: A systematic review and meta-analysis, Lancet, 382, 1039-1048, doi: 10.1016/s0140-6736(13)60898-3, 2013.

Shu, J., Dearing, J. A., Morse, A. P., Yu, L., and Yuan, N.: Determining the sources of atmospheric particles in Shanghai, China, from magnetic and geochemical properties, Atmos. Environ., 35, 2615-2625, doi: 10.1016/S1352-2310(00)00454-4, 2001.

Sofowote, U. M., Su, Y., Dabek-Zlotorzynska, E., Rastogi, A. K., Brook, J., and Hopke, P. K.: Sources and temporal variations of constrained PMF factors obtained from multiple-year receptor modeling of ambient $PM_{2.5}$ data from five speciation sites in Ontario, Canada, Atmos. Environ., 108, 140-150, doi: 10.1016/j.atmosenv.2015.02.055, 2015.

Strak, M., Janssen, N. A., Godri, K. J., Gosens, I., Mudway, I. S., Cassee, F. R., Lebret, E., Kelly, F. J., Harrison, R. M., Brunekreef, B., Steenhof, M., and Hoek, G.: Respiratory health effects of airborne particulate matter: The role of particle size, composition, and oxidative potential-the RAPTES project, Environ. Health. Perspect., 120, 1183-1189, doi: 10.1289/ehp.1104389, 2012.

Streit, B.: Lexikon der Ökotoxikologie, Wiley-VCH, Weinheim, Germany, 1991.

Strickland, M. J., Hao, H., Hu, X., Chang, H. H., Darrow, L. A., and Liu, Y.: Pediatric emergency visits and short-term changes in $PM_{2.5}$ concentrations in the U.S. State of Georgia, Environ. Health. Perspect., 124, 690-696, doi: 10.1289/ehp.1509856, 2016.

Suess, D. T.: Single particle mass spectrometry combustion source characterization and atmospheric apportionment of vehicular, coal and biofuel exhaust emissions, PhD, Chemistry, University of California, Riverside, CA, USA, 2002.

Tang, M., Huang, X., Lu, K., Ge, M., Li, Y., Cheng, P., Zhu, T., Ding, A., Zhang, Y., Gligorovski, S., Song, W., Ding, X., Bi, X., and Wang, X.: Heterogeneous reactions of mineral dust aerosol: Implications for tropospheric oxidation capacity, Atmos. Chem. Phys. Discuss., 2017, 1-124, doi: 10.5194/acp-2017-458, 2017.

Tao, L., Fairley, D., Kleeman, M. J., and Harley, R. A.: Effects of switching to lower sulfur marine fuel oil on air quality in the San Francisco Bay area, Environ. Sci. Technol., 47, doi: 10171-10178, 10.1021/es401049x, 2013.

Tchounwou, P. B., Yedjou, C. G., Patlolla, A. K., and Sutton, D. J.: Heavy metals toxicity and the environment. In Molecular, Clinical and Environmental Toxicology, 133-164, ISBN: 978-3-7643-8337-4, 2012.

Tian, H. Z., Zhu, C. Y., Gao, J. J., Cheng, K., Hao, J. M., Wang, K., Hua, S. B., Wang, Y., and Zhou, J. R.: Quantitative assessment of atmospheric emissions of toxic heavy metals from anthropogenic sources in China: Historical trend, spatial distribution, uncertainties, and control policies, Atmos. Chem. Phys., 15, 10127-10147, doi: 10.5194/acp-15-10127-2015, 2015.

Traversi, R., Becagli, S., Calzolai, G., Chiari, M., Giannoni, M., Lucarelli, F., Nava, S., Rugi, F., Severi, M., and Udisti, R.: A comparison between PIXE and ICP-AES measurements of metals in aerosol particulate collected in urban and marine sites in Italy, Nucl. Instrum. Meth. B, 318, 130-134, doi: 10.1016/j.nimb.2013.05.102, 2014.

Usher, C. R., Michel, A. E., and Grassian, V. H.: Reactions on mineral dust, Chem. Rev., 103, 4883-4940, doi: 10.1021/cr020657y, 2003.

Verma, V., Shafer, M. M., Schauer, J. J., and Sioutas, C.: Contribution of transition metals in the reactive oxygen species activity of PM emissions from retrofitted heavy-duty vehicles, Atmos. Environ., 44, 5165-5173, doi: 10.1016/j.atmosenv.2010.08.052, 2010.

Viana, M., Amato, F., Alastuey, A., Querol, X., Moreno, T., García Dos Santos, S., Herce, M. D., and Fernández-Patier, R.: Chemical tracers of particulate emissions from commercial shipping, Environ. Sci. Technol., 43, 7472-7477, 10.1021/es901558t, 2009.

Visser, S., Slowik, J. G., Furger, M., Zotter, P., Bukowiecki, N., Canonaco, F., Flechsig, U., Appel, K., Green, D. C., Tremper, A. H., Young, D. E., Williams, P. I., Allan, J. D., Coe, H., Williams, L. R., Mohr, C., Xu, L., Ng, N. L., Nemitz, E., Barlow, J. F., Halios, C. H., Fleming, Z. L., Baltensperger, U., and Prévôt, A. S. H.: Advanced source apportionment of size-resolved trace elements at multiple sites in London during winter, Atmos. Chem. Phys., 15, 11291-11309, doi: 10.5194/acp-15-11291-2015, 2015a.

Visser, S., Slowik, J. G., Furger, M., Zotter, P., Bukowiecki, N., Dressler, R., Flechsig, U., Appel, K., Green, D. C., Tremper, A. H., Young, D. E., Williams, P. I., Allan, J. D., Herndon, S. C., Williams, L. R., Mohr, C., Xu, L., Ng, N. L., Detournay, A., Barlow, J. F., Halios, C. H., Fleming, Z. L., Baltensperger, U., and Prévôt, A. S. H.: Kerb and urban increment of highly time-resolved trace elements in PM_{10},

$PM_{2.5}$ and PM_{10} winter aerosol in London during ClearfLo 2012, Atmos. Chem. Phys., 15, 2367-2386, doi: 10.5194/acp-15-2367-2015, 2015b.
Wang, F., Chen, Y., Meng, X., Fu, J., and Wang, B.: The contribution of anthropogenic sources to the aerosols over East China Sea, Atmos. Environ., 127, 22-33, doi: 10.1016/j.atmosenv.2015.12.002, 2016.
Wang, J., Hu, Z., Chen, Y., Chen, Z., and Xu, S.: Contamination characteristics and possible sources of PM_{10} and $PM_{2.5}$ in different functional areas of Shanghai, China, Atmos. Environ., 68, 221-229, doi: 10.1016/j.atmosenv.2012.10.070, 2013a.
Wang, X., Bi, X., Sheng, G., and Fu, J.: Hospital indoor PM_{10}/$PM_{2.5}$ and associated trace elements in Guangzhou, China, Sci. Total Environ., 366, 124-135, doi: 10.1016/j.scitotenv.2005.09.004, 2006.
Wang, X., Williams, B. J., Wang, X., Tang, Y., Huang, Y., Kong, L., Yang, X., and Biswas, P.: Characterization of organic aerosol produced during pulverized coal combustion in a drop tube furnace, Atmos. Chem. Phys., 13, 10919-10932, doi: 10.5194/acp-13-10919-2013, 2013b.
West, J. J., Cohen, A., Dentener, F., Brunekreef, B., Zhu, T., Armstrong, B., Bell, M. L., Brauer, M., Carmichael, G., Costa, D. L., Dockery, D. W., Kleeman, M., Krzyzanowski, M., Kunzli, N., Liousse, C., Lung, S. C., Martin, R. V., Poschl, U., Pope, C. A., 3rd, Roberts, J. M., Russell, A. G., and Wiedinmyer, C.: "What we breathe impacts our health: Improving understanding of the link between air pollution and health", Environ. Sci. Technol., 50, 4895-4904, doi: 10.1021/acs.est.5b03827, 2016.
WHO (World Health Organization) Air quality guidelines - global update 2005, available online at http://www.who.int/phe/health_topics/outdoorair/outdoorair_aqg/en/, 2005. (last accessible: 7/7/2017)
Wu, Q. R., Wang, S. X., Zhang, L., Song, J. X., Yang, H., and Meng, Y.: Update of mercury emissions from China's primary zinc, lead and copper smelters, 2000-2010, Atmos. Chem. Phys., 12, 11153-11163, doi: 10.5194/acp-12-11153-2012, 2012.
Yanca, C. A., Barth, D. C., Petterson, K. A., Nakanishi, M. P., Cooper, J. A., Johnsen, B. E., Lambert, R. H., and Bivins, D. G.: Validation of three new methods for determination of metal emissions using a modified Environmental Protection Agency Method 301, J. Air Waste Manage. Assoc., 56, 1733-1742, doi: 10.1080/10473289.2006.10464578, 2006.
Yu, S.: Water spray geoengineering to clean air pollution for mitigating haze in China's cities, Environ. Chem. Lett., 12, 109-116, doi: 10.1007/s10311-013-0444-0, 2014.
Zhang, X., Hecobian, A., Zheng, M., Frank, N. H., and Weber, R. J.: Biomass burning impact on $PM_{2.5}$ over the southeastern US during 2007: integrating chemically speciated FRM filter measurements, MODIS fire counts and PMF analysis, Atmos. Chem. Phys., 10, 6839-6853, doi: 10.5194/acp-10-6839-2010, 2010.
Zhao, J., Lewinski, N., and Riediker, M.: Physico-chemical characterization and oxidative reactivity evaluation of aged brake wear particles, Aerosol Sci. Technol.,

49, 65-74, doi: 10.1080/02786826.2014.998363, 2015.
Zhao, M., Zhang, Y., Ma, W., Fu, Q., Yang, X., Li, C., Zhou, B., Yu, Q., and Chen, L.: Characteristics and ship traffic source identification of air pollutants in China's largest port, Atmos. Environ., 64, 277-286, doi: 10.1016/j.atmosenv.2012.10.007, 2013.
Zhen, L., Li, M., Hu, Z., Lv, W., and Zhao, X.: The effects of emission control area regulations on cruise shipping, Transport. Res. D-Tr. E., 62, 47-63, doi: 10.1016/j.trd.2018.02.005, 2018.
Zheng, J., Tan, M., Shibata, Y., Tanaka, A., Li, Y., Zhang, G., Zhang, Y., and Shan, Z.: Characteristics of lead isotope ratios and elemental concentrations in PM_{10} fraction of airborne particulate matter in Shanghai after the phase-out of leaded gasoline, Atmos. Environ., 38, 1191-1200, doi: 10.1016/j.atmosenv.2003.11.004, 2004.